Durable High Surface Area Electrodes for Rechargeable Zinc Air Batteries

by

Raihan Ahmed

A thesis

presented to the University of Waterloo

in fulfillment of the

thesis requirement for the degree of

Master of Applied Science

in

Chemical Engineering

Waterloo, Ontario, Canada, 2015

Author's Declaration

I hereby declare that I am the sole author of this thesis. This is a true copy of the thesis, including any required final revisions, as accepted by my examiners.

I understand that my thesis may be made electronically available to the public.

Abstract

The fast growth in technology has led to an increase in demand for convenient storage of energy, primarily rechargeable batteries. People have shown significant interest in metal air batteries throughout history due to their high energy storage capacities, safety, and low cost. These batteries do not require the oxygen, one of their constituent fuels, to be stored inside the cell leading to high volumetric capacities. This is achievable due to the utilization of a unique gas diffusion electrode system that has a complex three phase interface regime. One of the safest and cheapest from the metal air family is the zinc air battery, zinc being one of the most abundant metals on earth. However, researchers have come across various challenges when dealing with these batteries and some of them include sluggish reaction rates, slow gas diffusion rates, and cell material degradation leading to poor power densities and charge-discharge cyclability. This work will address some of these issues via electrode and cell design optimization utilizing some of the proprietary technologies developed in the Applied Nanomaterials and Clean Energy Laboratory.

In this work, it has been demonstrated that highly conductive and porous zinc electrodes can be developed that eliminate some of the detrimental dendrite formations usual in conventional zinc based batteries as well as increasing cell energy efficiency by 30% compared to conventional bulk zinc electrodes. These electrodes have been made by the use of nanomaterial templates and micellar voids as well as controlled temperature treatments to make strong porous structures making them ideal for use in commercial zinc air batteries. Not only that, extremely thin zinc anodes can be made by using zinc foam supports which can be ideal to acquire high C rates viable for use in vehicles.

Novel gas diffusion electrodes have also been developed which have very slow rates of passivation in alkaline electrolyte compared to conventional carbon gas diffusion electrodes. These novel gas diffusion electrodes are made using a modified roll pressing method which has been optimized to account for low cost large scale production and porosity ideal for high gas diffusion rates without compromising electrode hydrophobicity and clogging by electrolyte. Additives have been experimented with to make a compact stable bi-functional electrode unlike uni-functional charge and discharge cathodes that increase cell size. These additives have been fine tuned for high oxygen reduction and evolution reactions, sufficient hydrophobicity to prevent electrolyte clogging, and durability.

Cell designs have also been investigated and proposed, ideal for housing the proprietary anodes and cathodes that are leak proof, compact, and recyclable. They are easy to assemble in a stack and also address issues such as pressure buildup due to oxygen evolution. Each cell benefits from ample cathode area exposure to oxygen and a stack design that makes sure there is sufficient flow of air to the cells to maximize power density.

Acknowledgement

I would like to thank Dr. Zhongwei Chen for his guidance and support throughout my Master's Program. Also, I would like to express my gratitude to my thesis reviewers Dr. Zhongwei Chen, Dr. Aiping Yu, and Dr. Michael Fowler.

Special thanks go to my colleagues in our zinc air research group whose hard contribution and team work has made it possible to develop all the zinc air technologies in our lab. Ali Ghorbani, Dong Un Lee, Jayeon Choi, Hey Woong Park, Moon Gyu Park and Hao Liu has been amazing colleagues in providing guidance and help in many of my research projects.

Other colleagues such as Abdul Rahman Ghannoum, Rasim Batmaz, Pouyan Zamani, Fathy Hassan, Kun Feng and Ariful Haque have supported me mentally and contributed to the amazing experiences I had in my Master's study journey.

Table of Contents

List of Figures

List of Tables

1. Introduction

Since the start of the industrial revolution, the rapid growth in population [1] was accompanied with an increase in the use of fossil fuels such as oil, coal and natural gas, and natural energy such as hydropower and solar power. Fossil fuels and natural energy are collectively called primary energy. The consumption of primary energy was significant from the start of the industrial revolution and increased greatly which can be clearly seen in Figure 1.

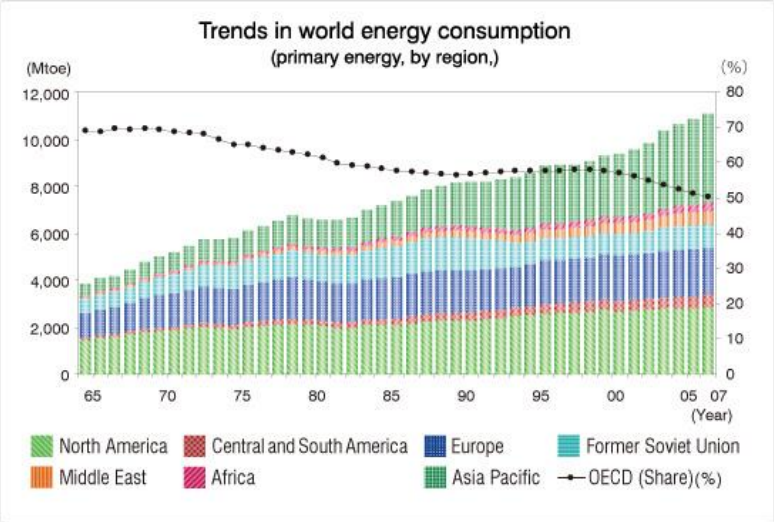

Figure 1. Primary Energy Consumption [2]

The growth in technology as well as population has led to the search for more convenient forms of storage of energy so that it can be easily distributed to the demanding population. Not only that, there have been growing concerns with the vast usage of fossil fuels leading to environmental pollution [3-4]. One likely solution is the use of renewable energy and to store these forms of unreliable energy into secondary energy [5]. Secondary energy is an energy

carrier and normally takes the form of batteries and fuel cells. Battery is a device that has predetermined stored chemical energy which can be changed into electrical energy [6-8]. Fuel cells are very similar with the only difference being that the chemical fuels need to be continuously input into the cells. Fuel cells and batteries contain a positive terminal called a cathode and a negative terminal called an anode. There is an electrolyte present which contain ions and allow the free flow of ions between terminals. Current flows through a load when connected to the terminals and this is due to a redox reaction that occurs at the terminals. Oxidation occurs at the anode whereas reduction occurs at the cathode during discharge.

Another important difference between batteries and fuel cells is the fact that some batteries can be rechargeable. Therefore, batteries can be classified into two categories: primary and secondary. Primary batteries are not rechargeable. Once the reactions occur, it cannot be reversed to regenerate the starting fuels. Secondary batteries, on the other hand, can be recharged by inputting electrical energy into the cells. The most common secondary batteries known are lithium ion, lead acid, nickel metal hydride, and nickel cadmium. Nickel metal hydride is known for its very high leakage leading to a poor lifetime. Lithium ion is currently a staple for use in portable electronics and hybrid electric vehicles due to its high energy and power density, great cyclability and very minimal leakage [8, 9, and 10]. However, its energy density of 300Wh/kg is significantly low compared to 1700Wh/kg which is that of gasoline [11]. This makes it challenging to commercially implement lithium ion batteries in electric vehicles and grid energy storage. A potential solution is the implementation of metal air batteries, particularly the zinc air battery, which have significantly higher energy densities, lower costs, and environmentally greener.

2. Rechargeable Zinc-air Batteries

Zinc is one of the most common metals, others being iron, aluminum, and copper. Zinc has many attractive properties as an electrical storage medium. Zinc used in electrical cells provides high energy density, stable and simple reaction kinetics and reversibility. Zinc air batteries are promising forms of energy storage devices that are cheap and have high energy density. The first metal air batteries were developed by Leclanche which used carbon based manganese dioxide air electrodes [12]. The main advantage of metal air batteries over other batteries is high energy density. This is due to the fact that one of the fuels of the battery does not need to be stored in it, and can be accessed from the surrounding air. It uses oxygen as one of its fuels.

The advantage of zinc air battery over some of the other popular batteries can be easily demonstrated from the chart in Figure 2. The chart shows the weight, volume and cost of a 48V 20Ah pack. These were calculated using approximate literature values of specific energy, energy density, and commercial cell cost. It is clearly evident that zinc air battery gives the best bang for the buck in terms of specific energy and energy density. Zn air has a nominal voltage of 1.6V, specific energy of 1000Wh/kg, specific capacity of 820mAh/g and specific power of 100W/kg [13]. Their specific energy is considerably large compared to that of lithium ion (300Wh/kg) making them an excellent alternative to the current inefficient batteries.

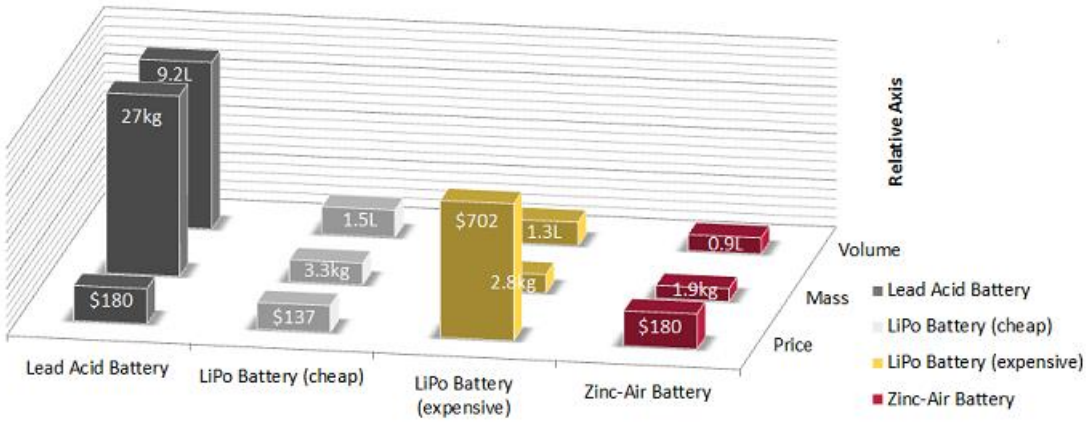

Figure 2. 48V 20Ah Battery Pack Comparison

Table 1 summarizes the characteristics of some metal air batteries. Li, Ca, Mg, and Al based metal air batteries are extremely voltage inefficient due to high anode passivation making it difficult to stabilize cell capacity. Zn is the most promising out of all the metal air batteries due to the metals abundancy, reaction stability, and most importantly, reversibility. The reason why it's reactions are reversible is due to the presence of a stable intermediate species called zincate [$Zn(OH)_4^{2-}$] which is a soluble version of ZnO in alkaline electrolyte. Iron air, on the other hand, forms iron (II) hydroxide during discharge which is hardly soluble and unable to form a reduced species like zincate.

Table 1. Metal Air Battery Characteristics [14]

Anode Metal	Specific Capacity (Ah/kg)	Theoretical Voltage (V)	Practical Voltage (V)
Li	3861	3.3	2.4
Ca	1337	3.4	2.0
Mg	2205	3.1	1.4
Al	2980	2.7	1.6
Fe	960	1.3	1.0
Zn	820	1.6	1.1

The electrochemical reactions of a typical zinc-air battery are shown in the equations below and demonstrated in Figure 3:

Anode: $Zn + 4OH^- \rightarrow Zn(OH)_4^{2-} + 2e^-$ ($E_0 = -1.25V$)

Fluid: $Zn(OH)_4^{2-} \rightarrow ZnO + H_2O + 2OH^-$

Cathode: $1/2\ O_2 + H_2O + 2e^- \rightarrow 2OH^-$ ($E_0 = 0.35V$)

Overall: $2Zn + O_2 \rightarrow 2ZnO$ ($E_0 = 1.6V$)

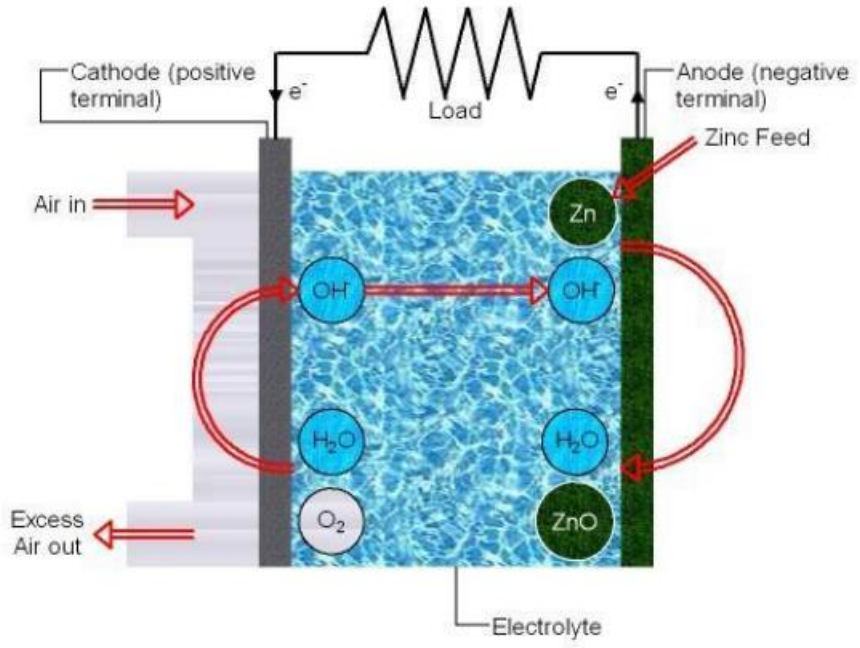

Figure 3. Rechargeable Zinc-air Cell Overview [15]

Zinc-air cells are composed of three parts; zinc metal as an anode, an air electrode as the cathode, which is divided into a gas diffusion layer and a catalyst active layer, and potassium hydroxide as electrolyte, as shown in Figure 3. Oxygen from the atmosphere diffuses into the porous carbon electrode by difference in pressure of oxygen between the outside and inside

of the cell, and then the catalyst facilitates the reduction of oxygen to hydroxyl ions in the alkaline electrolyte with electrons generated from the oxidation of zinc metal as the anode reaction. This is why it is called the three-phase reaction: catalyst (solid), electrolyte (liquid), and oxygen (gas) [16].

Zinc air has many challenges which need to be addressed in order to fully transition it into the commercial market. Fluidic Energy, which is based in Scottsdale, Arizona, is the only company that is commercially selling rechargeable zinc air batteries as of 2014. They supply units as an alternative for lead acid batteries and diesel generators in grid energy storage [17]. Their units utilize ionic liquids as the electrolyte. Couple of challenges of zinc air batteries has been listed below:

- Dendrite at the zinc anode considerably reduces the lifetime of the battery;
- High self-discharge due to zinc passivation;
- Low cell efficiencies due to hydrogen evolution;
- Sluggish oxygen reduction reactions leading to low power densities;
- Low cell lifetime due to degradation of air cathode at high currents;
- Carbon corrosion and zinc carbonate formation leading to electrolyte and cathode poisoning; and,
- Electrolyte drying out leading to slow diffusion kinetics.

Many of these challenges will be explained and addressed in the following sections. To overcome these challenges, one would need to understand the electrochemical and interfacial phenomena involved in these systems.

2.1. Zinc Electrode

Zinc metal forms the anode for zinc air batteries. During discharge, the metal oxidizes to zinc oxide. This involves a two-step reaction where the zinc first reacts with hydroxyl ions to form soluble zincate, which then loses water to the electrolyte and precipitates to zinc oxide. This phenomenon, where the solid metal first forms a soluble species followed by an insoluble one, is responsible for the detrimental shape change that occurs in the anode after repeated charge-discharge cycles. The shape change manifests into needle like dendrites which keep extending from the anode as shown in Figure 4.

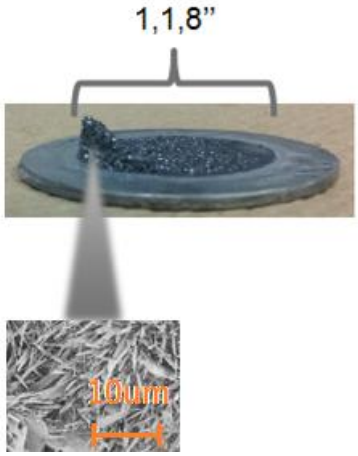

Figure 4. Zinc Anode Dendrites [18]

The coin in the figure is a bulk zinc plate that was cycled in a test zinc air cell. The coin was placed vertically when assembled in the cell; hence the dendrites accumulate at the bottom corner of the coin due to gravity. Eventually, these dendrites puncture the separator bridging between the anode and cathode and may lead to cell short circuiting. Dendrite formation is inevitable and cannot be fully prevented. However, increasing porosity of the anode can

significantly reduce outer surface dendrite formation by consolidating many of the dendrites formed to be inside the pores of the anode. This makes the anode last for much longer before losing its working capacity.

There are many ways this can be achieved without significantly compromising for anode structural integrity. One way is to incorporate cellulose into the anode [19]. The cellulose acts as tunnels in the anode which can absorb electrolyte. This is possible due to the fact that cellulose walls are highly hygroscopic. Another way to greatly reduce dendrite formation is to make ceramic anode. This zinc oxide anode is made very much like industrial ceramic. Zinc oxide powder is consolidated into pellets that are incorporated with some pore forming agents [20]. Then, the pellets are passed through several steps of changing temperature to sinter and strengthen the anode forming a structurally strong and porous ceramic anode.

Hydrogen evolution is one of the major culprits responsible for loss of energy efficiency in rechargeable zinc air batteries. The fact that the reduction potential of hydrogen evolution is 0.4V higher than that of zincate reduction in basic solution means that reduction of electrolyte is inevitable during charging. The equations below show the difference between zincate reduction and electrolyte reduction [21]:

$Zn + 4OH^- \rightarrow Zn(OH)_4^{2-} + 2e^- \ (E_0 = -1.25V)$

$H_2 + 2OH^- \rightarrow 2H_2O + 2e^- \ (E_0 = -0.85V)$

Hydrogen evolution is an unwanted reaction as it greatly reduces the charging efficiency of the cell. A higher voltage is required to charge the zinc oxide back to zinc as some of the

energy is wasted in hydrogen evolution. However, hydrogen evolution can be greatly reduced by alloying the zinc with heavy metals such as lead and cadmium. Due to the environmental and health effects of heavy metals, alloying is done with other metals such as indium and bismuth which are just as effective in increasing the over-potential of hydrogen evolution [22-24]. The only disadvantage of indium and bismuth are their costs; therefore, optimization of indium and bismuth alloying is critical to make sure they are kept at the minimum. Other ways would be to add additives to the electrolyte such as citric acid, indium and bismuth hydroxide, and other polymers that serve similar functions [25]. Adding additives, however, can greatly change the properties of the electrolyte such as ionic conductivity, viscosity, etc. and therefore, needs to be finely tuned.

2.2. Electrolyte and Separator

The electrolyte used in zinc air batteries need to harbor OH^{-1} ions. It is crucial for the anode and cathode reactions to occur in a basic environment to maintain low cathode over-potentials. Electrolytes include potassium hydroxide, sodium hydroxide and lithium hydroxide [26]. Potassium hydroxide is the most commonly used in zinc air batteries due to its stability and high ionic conductivity ($73.5\Omega^{-1}cm^2$) [27].

The concentration of KOH is very important in the performance of the cell. Low concentration of OH^{-1} ion may hamper the amount of reaction that takes place in the cell. OH^{-1} ions are required for both anode and cathode reactions. Not only that, the saturation concentration of zincate ions is directly proportional to the amount of OH^{-1} ions present in the

electrolyte. This is because two hydroxyl ions and a water molecule are required to form a zincate species from ZnO. Formation of zincate species is an intermediate crucial step to facilitate the reduction and oxidations occurring at the anode. Therefore, higher the saturation concentration allowed for zincate species, faster the rate of reaction. On the other hand, very high electrolyte concentrations can significantly increase the viscosity of the electrolyte, leading to lower diffusion rates for ions. The optimal concentration of pure KOH without any additives added was found to be 6M [28].

One huge disadvantage of basic liquid electrolytes is the formation of carbonate species due to presence of CO_2 in air that seeps into the cell [14]. The reaction is as follows:

$$CO_2 + 2KOH \rightarrow K_2CO_3 + H_2O$$

This precipitation of carbonate species in the electrolyte significantly reduces ionic conductivity in the electrolyte as well as blocking pores in the separator and cathode diffusion membrane. Not only that, it can also lead to flooding of the electrolyte in the cathode as it significantly makes the cathode hydrophilic. A couple of ways to prevent CO_2 precipitation is via use of a scrubber that is normally a chemical, such as LiOH, that absorbs all the CO_2 from air before it reaches the cathode. Another issue with liquid electrolyte is the dangers of leakage through a punctured cathode but this problem can be solved by addressing the cathode rather than the electrolyte.

There is extensive research being doing to replace liquid electrolyte with a solid or gel electrolyte. Gel electrolytes can be advantageous as the electrolyte does not have the

tendency to dry out. However, the increased viscosity can significantly reduce ionic diffusion and researchers are attempting to increase ionic diffusion. Solid electrolytes are also being researched and their main advantage is the absence of electrolyte leakage and carbonate species formation.

There are two kinds of solid electrolytes: anion exchange polymer membrane and ceramic membrane. The anion exchange membrane consists of a polymer chain which is functionalized with cationic groups such as sulfonium. These cationic groups facilitate OH^{-1} transfer; however, they are susceptible to nucleophilic attack by Hoffman elimination at β hydrogen sites leading to membrane degradation over time. Also, these anion exchange membranes have very low ionic conductivities compared to liquid electrolyte. Ceramic membranes are very similar in the fact that they also have low ionic conductivities and helps transfer OH^{-1} ions via positive sites. An example of a ceramic membrane is SnP_2O_7 where the Sn (+4 valence electrons) is partially replaced by +5 valence elements [29]. The slightly positive charge will help facilitate transfer of OH^{-1} ions. For the thesis' research, 6M liquid KOH will be utilized for most of the tests and experiments as it is easier to use standard electrolyte for comparison of different electrodes.

Separators are mechanical membranes that prevent short circuits in the cell. They separate the anode and cathode compartments and prevent solid particles from passing through. Therefore, it is crucial for separators to have an optimized pore size that can prevent solid particles from passing through but allowing free ion transfer. An important function of separators is preventing dendrites formed to contact the cathode. However, the dendrites can eventually puncture through separators over time and lead to short circuiting. One example of

a separator is a polyethylene-polypropylene membrane. Celgard 5550 is a commercial mechanical separator that is normally used for zinc air batteries. For the purpose of this thesis' work, this membrane will be utilized for the tests and experiments.

2.3. Air Electrode

The air electrode which is normally called the gas diffusion electrode (GDE) is a three layer electrode system consisting of the following layers:

- Hydrophilic microporous layer consisting of catalyst particles. These catalyst particles can be bi-functional (responsible for catalyzing both oxidation and reduction) or uni-functional (reduction);
- Hydrophobic gas diffusion layer responsible for oxygen absorption and distribution to the catalyst sites in the hydrophilic layer; and,
- Current collector that evenly spans throughout the electrode to make sure over-potential is not localized at certain spots of the cathode.

When designing the hydrophilic layer, it is vital that the hydrophobic polytetrafluoroethylene binder is kept to a minimum to maximize electrolyte exposure at the catalyst sites. PTFE is the only suitable binder in the case of zinc air batteries due to its high corrosion resistance in basic electrolyte, as well as hydrophobic properties. The hydrophobic layer is designed in such a way to promote maximum gas intake without leading to electrolyte flooding. Electrolyte flooding will prevent oxygen reaching catalyst sites at the hydrophilic regime.

The hydrophobic layer characteristic is closely controlled by modifying the PTFE content. This will be explained further in the following sections using interfacial phenomena.

Current collectors are chosen based on conductivity and stability of a material. Nickel and stainless steel are highly conductive as well as corrosion resistant making them ideal for use only at the cathode. However, they cannot be used at the anode due to their interaction with the zinc anode. The oxides of nickel and iron oxide help catalyze hydrogen evolution. Therefore, when in contact with zinc, zinc passivates releasing hydrogen. The optimal current collector for the anode is copper which is less corrosion resistant but stable with zinc. Also, it has good affinity for zinc being evenly deposited on it during charging. It is the same reason why zinc and copper alloys together very well which is widely used for organic synthesis [30].

2.4. Understanding Air Electrode using Adsorption Models

Optimal use of oxygen in a zinc-air battery requires the air electrode to have both a highly porous structure (high surface area) and proper catalysts for oxygen reduction reaction (ORR). These two requirements should be considered simultaneously for designing an air electrode. The mechanism of adsorption is very complicated and difficult to model because the electrode has a heterogeneous structure. The different layers of the electrode behave very differently. Before one can fabricate an optimal cathode, it is very crucial to understand the different interfacial phenomena that occur at the different layers of the cathode.

2.4.1. Gas Diffusion Membrane: BET Isotherm

A typical gas diffusion electrode is shown in Figure 5. The black particles in the diagram are the catalyst active sites. Non-noble metal catalysts include perovskite, pyrochlore, and spinel structured materials which have very high surface area. The large grey particles are the conducting or supporting material. These are generally carbon based conductive materials such as graphite, acetylene black, Vulcan XC-72, etc.

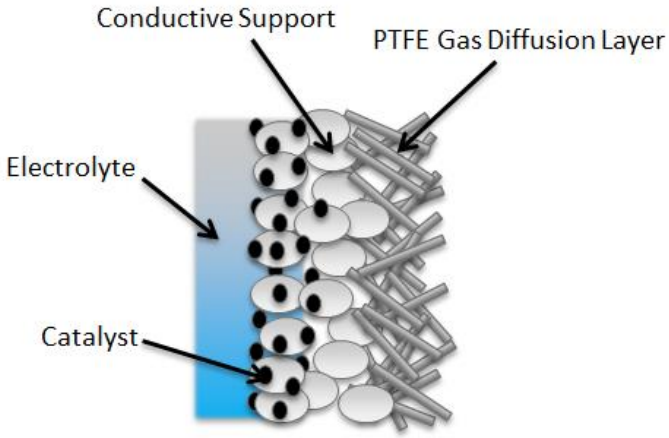

Figure 5. Schematic of a Typical Gas Diffusion Electrode

The matrix of catalyst and conductive support is maintained by PTFE binder. The sticks represent porous PTFE diffusion layer. This layer can have carbon species in it and generally have a higher PTFE content than that of the microporous layer. The fact that there are interfaces where the layers meet and can have varying composition in the interfaces make the electrode assembly heterogeneous. Also, the fact that each layer is porous in nature and can allow air and electrolyte to intermix make the adsorption phenomena very complex. However, simplifying the model is the first step in understanding this complex phenomenon.

There are certain areas in the electrode which can be approximately treated as homogenous. For example, the PTFE back layer constitutes a mesh like network of carbon species bridged by PTFE binder that is highly hydrophobic as shown in Figure 6 [31].

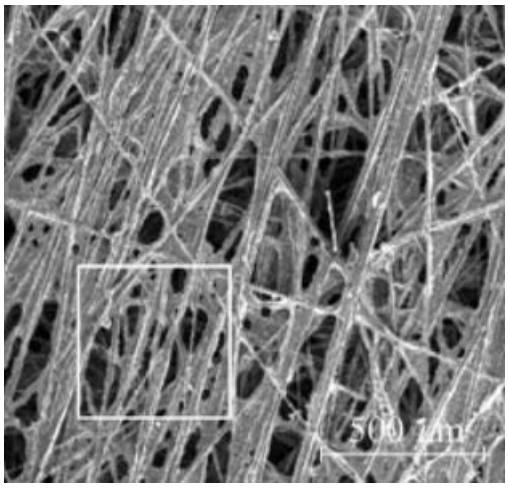

Figure 6. Gas Diffusion Layer [32]

The carbon species in Figure 6 are carbon fibers. The reason why this layer can be treated as a homogenous solid is due to the fact that PTFE and the carbon species share similar properties: very close bulk and true densities and high hydrophobic characteristic. The purpose of this back layer is to adsorb oxygen from the atmosphere but prevent electrolyte from the inside of the cell seeping out. This layer can be easily understood using the BET theory.

The BET method is based on a multilayer adsorption theory. The gas adsorbs on the surface of the gas diffusion network in multiple layers. One can measure the amount of gas being adsorbed at the surface at a given pressure and this will allow for the determination of the

surface area of the gas diffusion layer. Both total and active surface area of the gas diffusion layer can be found. The assumptions for the model are as follows:

- The network of carbon and PTFE is approximated as a homogeneous surface;
- There is no lateral interaction between the different molecule species;
- Interaction of gas is taken into account only for oxygen in air. Other species are ignored;
- The topmost gaseous layer is approximated to be in equilibrium with the vapor phase;
- First layer: Heat of adsorption; Higher layers; Heat of condensation; and,
- At saturation pressure, the number of layers becomes infinite.

The adsorption phenomenon is the direct consequence of surface energy. The energy is minimized in the bulk because every atom/molecule is surrounded by neighbors. However, in the case of a surface, the high energy leads to an affinity for neighboring gaseous molecules. The typical equation for BET is as follows:

$$\frac{1}{v[(\frac{p_0}{p})-1]} = \frac{c-1}{v_m c}\left(\frac{p}{p_0}\right) + \frac{1}{v_m c} \tag{1}$$

The constants p and p_0 are the equilibrium and saturation pressure of oxygen at the temperature of adsorption, v is the amount of oxygen adsorbed, v_m is the monolayer of oxygen adsorbed, and c is the BET constant. Figure 7 shows a general BET adsorption isotherm.

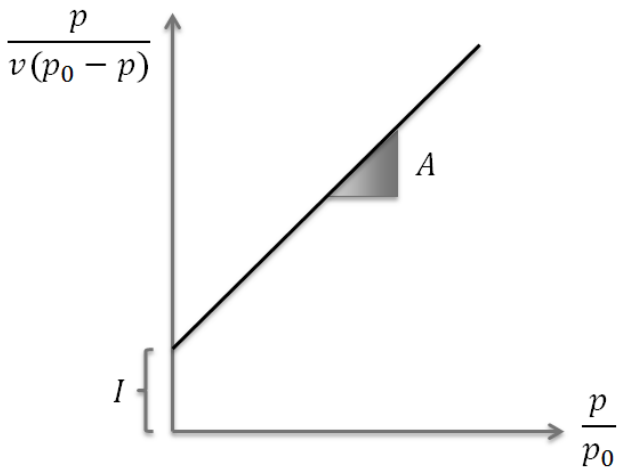

Figure 7. Typical BET Isotherm Plot

One can find v_m and c using the following equations:

$$v_m = \frac{1}{A + I} \tag{2}$$

$$c = 1 + \frac{A}{I} \tag{3}$$

The constants A and I are the slope and intercept of the BET isotherm curve. The total surface area (S_{total}) and specific surface area (S_{BET}) can be found using the following equations:

$$S_{total} = \frac{v_m N s}{V} \tag{4}$$

$$S_{BET} = \frac{S_{total}}{a} \tag{5}$$

The constants N and s are the Avogadro's number and cross section of the adsorbate. V, on the other hand, is the molar volume of oxygen adsorbed and a is the approximate mass of the adsorbing region [33].

As one moves from the homogenous regime to the heterogeneous regime, the model gets more complicated as it becomes a three phase interface. At the center of the electrode assembly which constitutes the interface between the hydrophilic and hydrophobic regime, the hydroxyl ions, water, oxygen, catalyst, PTFE, and support, all take part in a complex chemisorption/physisorption process. Active research in this field includes finding the right formula of the above chemicals such that the three phase interface reaction regime is at an ideal spot of the gas diffusion electrode.

Too much PTFE content can prevent electrolyte from reaching the reaction sites leading to water/hydroxyl ion limited reaction rates. On the other hand, loading the electrode with water loving active catalyst material can lead to full flooding of the electrode which essentially reduces the overall oxygen concentration in the electrode. The case is the same for the absence of PTFE which greatly reduces hydrophobic characteristic of the electrode. Not only that, the phenomenon becomes more complicated when recharging reactions is added to the picture. Recharge reverses the reaction equations which means that the active sites need to release byproducts (oxygen and water), which can possibly introduce electrolyte into the hydrophobic gas diffusion layer [34]. The function of PTFE can be summed up simply with Figure 8.

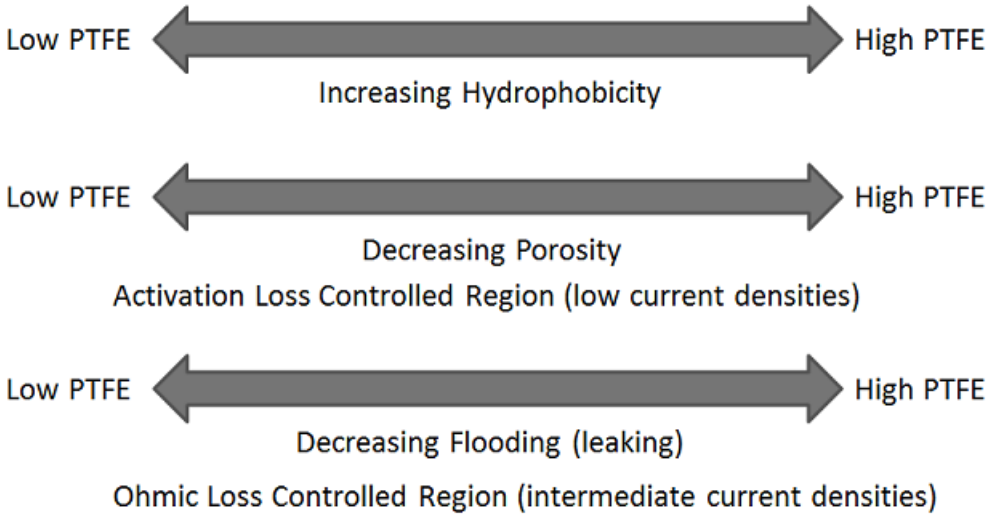

Figure 8. Effect of PTFE on Cathode Properties

At low current densities, the major contribution of PTFE content is to the degree of hydrophobicity and porosity. Increasing PTFE content in the electrode reduces porosity; however, hydrophobicity is increased. This is called the activation loss controlled region. At higher current densities, the ohmic loss controlled region takes over. In this region, there is more generation of water at the cathode leading to higher chance of flooding. Therefore, a high PTFE content, which increases hydrophobicity, is required to prevent this flooding. It is important to note that this does not occur during discharge. However during charge, there is production of water at the oxygen electrode leading to leaking at the gas diffusion layer. The best PTFE content is 20wt% if both the benefits of activation and ohmic loss controlled regions are taken into consideration. This ensures a balance between porosity and hydrophobicity.

It is important to note that the PTFE content is based on a GDL composed of purely carbon with a true density of 1.9g/cm^2 and apparent density of 0.3g/cm^2. Therefore, the optimal

weight percentage of PTFE will slightly vary for cathodes with different amounts of catalyst, and a huge variation for cathodes which are made of other support materials. One way to make sure the contribution of PTFE to cathode characteristics is consistent is by utilizing volume percentages. This will keep the amount of volume in the cathode occupied by PTFE consistent, as well as the other materials. Surface properties are a function of space rather than weight and utilizing volume percentages will make the cathode independent of varying material densities.

2.4.2. Chemisorption at the Catalyst Active Sites

It is well known that the kinetics of the oxygen reduction reaction (ORR) is very sluggish and that over-potential is required for the desired reaction. Power density and current rates are affected as a result. As the current is increased, the over-potential increases. The same is true for oxygen evolution reaction (OER); in fact, to a greater degree. Excellent ORR catalysts such as platinum on carbon support and high surface area electrolytically precipitated MnO_2 exist. However, these high performing catalysts degrade and lose its performance quickly in OER conditions. Efforts need to be made to overcome this problem by finding proper catalysts that are bi-functional in nature reducing both the charging and discharging over-potential. Figure 9 shows a typical charge and discharge curve of a zinc air cell.

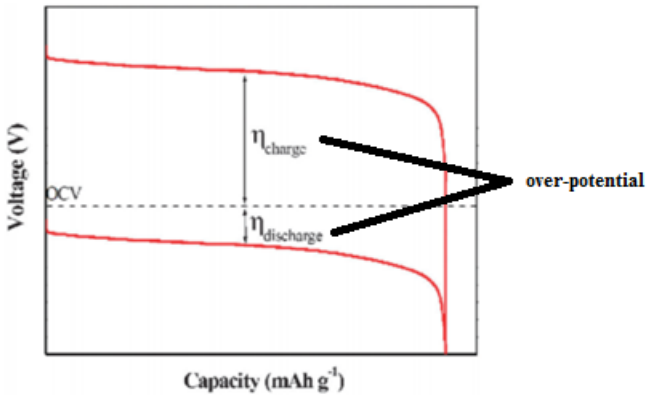

Figure 9. Over-potential

Reproduced from [35] with permission of The Royal Society of Chemistry.

It can be seen that the operating voltage is lower during discharge and higher during charge compared to that of open circuit. Research is done in the lab to synthesize novel bi-functional catalysts that reduce these over-potentials; therefore, increasing cell efficiency. However, this is not the focus of this thesis and thus, this work will solely deal with cathode and anode fabrication.

Well known candidates for the catalyst are transition metal oxides with a 3D nanostructure such as perovskite, pyrochlore and spinel. However, these catalysts only perform optimally in composite form along with an ORR catalyst. Common examples would be cobalt (II, III) oxide nanowires with nitrogen doped carbon nanotubes as composite or core corona structured lanthanum nickel oxide with nitrogen doped carbon nanotubes as the corona. These catalysts have been developed in the lab and are able to achieve low over-potentials and long cycle lifetime without degradation. However, for the purpose of this thesis' experiments, standard MnO_2 and Co_3O_4 nanoparticles manually mixed with sub-optimal

ORR catalyst such as functionalized multi-walled carbon nanotubes or activated charcoal will be utilized. This is to ensure contribution of catalyst is kept consistent throughout so that fabrication techniques can be investigated.

Catalyst active materials are normally hydrophilic in nature with a high surface energy so that it attracts water molecules. Oxygen molecules are attracted to these sites by adjacent PTFE and carbon material that are hydrophobic in nature. These oxygen molecules adsorb to the active catalyst and get reduced via a 1 or 2 step four electron reduction processes. For non-noble metal catalysts such as manganese and cobalt oxide, the latter is normally the case. Each oxygen atom coordinates to the catalyst and allows one electron to transfer leading to the 2 electron reduction of oxygen to peroxide ions [36].

1 Step Reduction: $O_2 + 2H_2O + 4e^- \rightarrow 4OH^-$ ($E_0 = 0.40V$)

2 Step Non-rate Limiting: $O_2 + H_2O + 2e^- \rightarrow HO_2^- + OH^-$ ($E_0 = -0.07V$)

2 Step Rate Limiting: $HO_2^- + H_2O + 2e^- \rightarrow 3OH^-$ ($E_0 = 0.87V$)

Decomposition: $2HO_2^- \rightarrow 2OH^- + O_2$

The two electron reduction of peroxide ions to hydroxyl ions is the rate limiting step. The mechanism of the reactions can be better understood by the mechanisms that occur when testing the catalysts using cyclic voltammetry. Cyclic voltammetry (CV) refers to cycling the potential between chosen low and high points and recording the current in the potential cycling region. The cycle is through a potential region in which a redox reaction of interest occurs. The instrument that produces the potential scan and records the current is called a potentiostat. It is used for a quantitative study of catalyst activity in the potential region of the

ORR. The electrode is assembled into a rotating apparatus that spin the electrode in the solution at fixed revolutions per minute values. This voltammetric technique is called rotating disk voltammetry (RDV), and the electrode is called a rotating disk electrode (RDE).

The rotating disk methodology provides a convenient means for characterizing the efficiency of an electro-catalytic material. Conventional electrode reaction happens in the absence of convection so that there is redox behavior of the species present and the natural diffusion of materials at the electrode surface. The migration is a result of concentration gradients that are formed at the electrode surface from electrode reactions at that surface. The migration of the species at the electrode surface behaves according to Fick's laws of diffusion. Diffusion is the dominant process for the transport of the species on the surface of an electrode immersed in a stagnant electrolyte solution. Therefore, to study the kinetic controlled current (current due to the activity of the catalyst) one must have full control on the diffusion current. Mass transport can be significantly improved by introducing forced convection. Rotating the electrode is an effective way to induce convection in a controlled manner. A rotating electrode drags fresh material from the bulk solution to the surface of the electrode and electrolyzed products are spun away into the bulk solution, as illustrated in Figure 10.

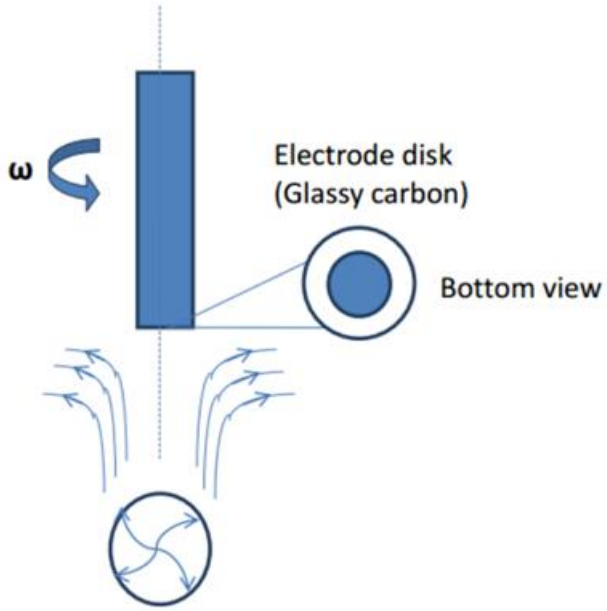

Figure 10. Rotating Disk Electrode [37]

In the entire potential sweeping region, the overall current i is related to i_k and i_d according to the Koutecky-Levich equation [37]:

$$\frac{1}{i} = \frac{1}{i_k} + \frac{1}{i_d} \tag{6}$$

The constants i_k and i_d are the kinetic and diffusion current respectively. i_d is directly proportional to $w^{\frac{1}{2}}$ where w is the angular frequency of rotation. Therefore, plotting a graph of i^{-1} versus $w^{-\frac{1}{2}}$ gives a straight line at constant temperature, with a slope that depends upon the diffusion coefficient D and an intercept from which the reactive rate constant k_f may be determined. The following equations relate i_d and i_k to D and k_f respectively [37]:

$$i_d = 0.62nFAD^{\frac{2}{3}}w^{\frac{1}{2}}v^{-\frac{1}{6}}C \quad (7)$$

$$i_k = nFAk_fC \quad (8)$$

The constant n is the number of electrons involved in the redox process, F is the Faraday constant, A is the surface area of the working electrode, D is the diffusion coefficient of the electroactive species in the bulk solution, w is the angular frequency of rotation, v is the kinematic viscosity of the electrolyte solution, k_f is the rate constant for desorption, and C is the concentration of the electroactive redox species in the bulk solution [37].

2.5. Non-idealities: Changing Surface Properties of PTFE; GDE Passivation

Wetting refers to when liquids contact solids and are able to maintain that. This is normally as a result of the type of intermolecular forces between the two. Depending on the presence of the type of forces present between the molecules, which include both adhesive and cohesive forces, the amount of wetting that occurs varies between liquids. However, this can be easily classified into two categories by explaining the type of solid surfaces that liquids interact with. These two main types of solid surfaces are high energy and low energy solids surfaces. The energy of these solid surfaces is dependent on the forces present between the molecules of these solids.

High energy solids are normally ceramics, glasses, and metals. This is because the forces present between the molecules that hold them together are strong forces such as covalent, ionic, and metallic. Low energy solids are hydrocarbons, fluorocarbons, other organic compounds, etc. The type of forces holding these molecules together are normally very weak such as van der Waals and hydrogen bonding. Aqueous liquids will generally wet high energy solids because of polar interactions. The contact angle between the liquid and solid is below 90°C in this case. However, this is not always the case for low energy solids where the wetting could be either partial or full. Low energy solids that do not have any dipole moment to them are generally hydrophobic. The contact angles achieved for this kind of solids are above 90°C.

PTFE is classified as a very low energy solid. It is widely used as a super hydrophobic membrane and additive to prevent electrolyte seeping out of the cell in zinc-air batteries. However, its hydrophobicity can be affected due to various reasons leading to non-ideal cases. For example, it was reported that the hydrophobicity of the PTFE film is progressively reduced when it is soaked in a solution of KOH [38]. This means that over time, the electrolyte will be able to wet the PTFE present in the gas diffusion layer. This will lead to flooding of the gas diffusion layer, neutralizing the adsorption of air into the electrode and rendering the cell dead. As shown in Figure 11, the contact angle decreased with the duration of soaking in KOH solution. Still pictures were taken at time frames: 0h, 72h, and 148h. It can be seen that the droplets slowly lose contact angle over time.

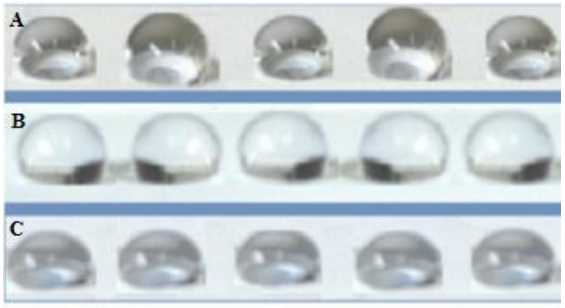

Figure 11. Image of KOH Droplets on PTFE at Different Time Intervals; A) Before Soaking; B) After 72h Soaking; C) After 148h Soaking

Reproduced from [38] with permission of Electrochemical Science Group.

Another reason that could lead to the flooding is the effect of temperature on the electrolyte. It has been reported that KOH electrolyte loses its viscosity when the temperature is increased leading to an increase in its surface tension [38]. It is possible for zinc air batteries to generate heat in a practical setup where a battery has huge number of cells stacked together. This heat could increase the temperature of KOH in cells, decreasing its viscosity and surface tension. However, with the help of ventilation and cooling, the temperature rise in zinc air batteries can be mitigated preventing KOH flooding. Figure 12 shows how contact angle of a 6M KOH droplet is reduced when it is put on a PTFE film with a higher temperature. Still pictures were taken of the KOH droplet on PTFE film when it was at room temperature and after it was heated in a boiling water bath.

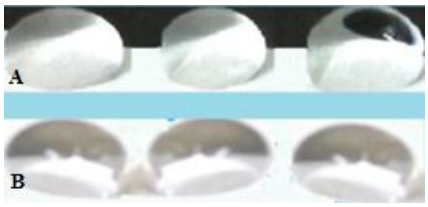

Figure 12. Image of KOH Droplets on PTFE at Different Temperatures; A) Room Temperature, B) Boiling Water Hot Bath

Reproduced from [38] with permission of Electrochemical Science Group.

Electro-osmosis is another cause for the flooding of liquid electrolyte in gas diffusion electrodes. However, this is not so much dependent on the current but more so on the sensitivity of the surface tension of a KOH solution to electricity. One might believe that the transport (leakage) of electrolytes/water is caused by the drag created by electrons or ions. However, tests conducted show that, when a power supply is connected to two porous conducting electrodes dipped in KOH and having the same electrolyte height, the positive electrode has a higher electrolyte height compared to the negative electrode [38]. One can conclude from this experiment that air cathodes have a high tendency to be wetted and vice versa for anodes. This is the complete opposite of what one would want for in zinc air batteries. It was also shown that the height of electrolyte is not affected by varying the voltage. In fact, changing the electrolyte solution from KOH to water affects the heights proving that it is a viscosity and surface tension based phenomenon. Therefore, it is crucial that the viscosity is kept to a minimum and one of the reasons why electrolyte additives are not a solution for many of the problems in zinc air batteries.

The supporting material of gas diffusion electrodes are always made of carbon. Examples of carbon support materials include graphite, Vulcan XC-72, acetylene black, etc. Reasons why

carbon materials are excellent supports are that they are cheap, have high electrical conductivity, and are extremely resistant to corrosion in basic environments. However, even though certain materials are corrosion resistant in basic environments, this is not always true when they are subject to extremely high potentials.

During charging, the applied potential difference between the cathode and anode in zinc air batteries can increase above 2V. The corrosion of high resistant materials is very evident at these voltages. It is even evident in the current collector which is usually stainless steel which develops a layer of red oxide formation after days of cathode charge-discharge cycling. The same is true for any carbon material present in the gas diffusion electrode which degrades and oxidizes to carbon dioxide when a charging voltage is applied [39]. This is a slow but visible process. Therefore, the commercially established carbon gas diffusion electrodes, which are very popular in fuel cells, cannot be used in rechargeable zinc air batteries. Fuel cells do not need to be charged unlike rechargeable zinc air batteries. Carbon degradation in carbon gas diffusion electrodes in zinc air batteries introduce gaping pores over time which can lead to electrode flooding and eventually, electrolyte leaking out of the cell from the cathode. The mechanism by which this happens is demonstrated in Figure 13.

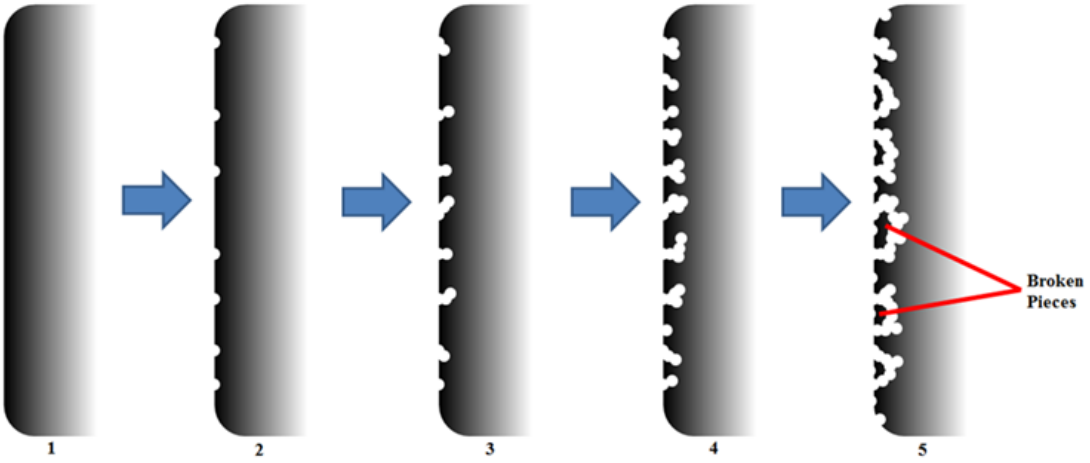

Figure 13. Carbon Corrosion in GDE

1. Fresh carbon cathode surface put in a high voltage charging environment.
2. Early signs of carbon corrosion showing loss of carbon from the surface due to oxidation to carbon dioxide.
3. Further carbon corrosion starting to make gaping pores.
4. The pores get wider and start to tunnel through the cathode, possibly leading to electrolyte leakage and flooding at the cathode.
5. Tunnels network and weaken structural integrity of the cathode, leading to chunks of cathode falling off into the electrolyte.

All these steps are confirmed by experiments conducted in the lab via use of commercial cathodes. All commercial cathodes tested to date have shown signs of leaking after charge-discharge cycling and discoloration of the electrolyte as shown in Figure 14.

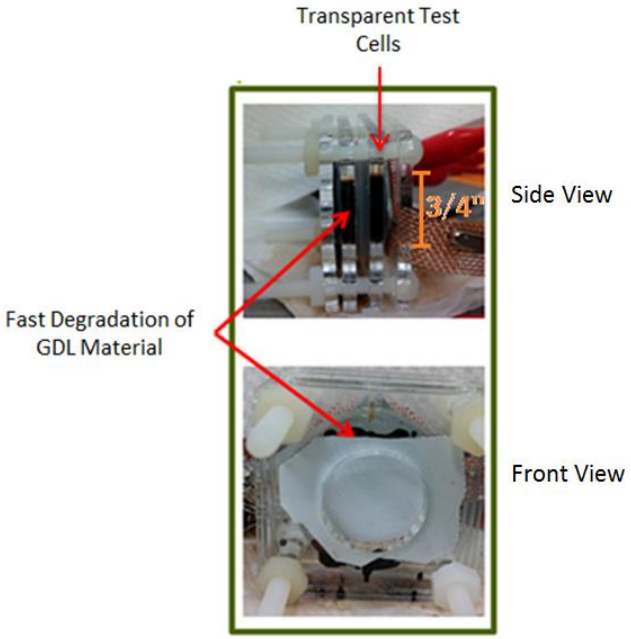

Figure 14. Electrolyte Discoloration from Carbon Degradation during Cycling

Carbon leeching off into the electrolyte is a major issue in the performance of the cell as it greatly increases the viscosity of the electrolyte reducing ionic diffusion. For all the reasons explained, carbon gas diffusion electrodes, even though still useful in primary zinc air batteries, are unsuitable for use if they need to be rechargeable. The gas diffusion electrodes have been a major setback in the commercialization of zinc air batteries. Therefore, it is crucial that a new cathode be designed primarily for rechargeable zinc air batteries that utilize other support materials.

3. Research Scope and Objectives

The research work in the thesis will deal mostly with fabrication techniques that will try to address many of the challenges stated previously for zinc air batteries. However, new catalyst synthesis will not be addressed as high performing catalysts such as core corona structured $LaNiO_3$-NCNT and cobalt oxide nanowires have already been developed in the lab, which give discharging voltages of about 1.2V and charging voltages of about 2V at 10mA/cm^2 current applied at cathode surface. The limiting factor now is not so much the catalyst but the actual structure of the anode and cathode. The following parts will be designed to address certain zinc air battery problems:

3.1. Porous Cellulose and Ceramic Anode

Highly porous zinc anodes will be fabricated. Balance between porosity and mechanical strength will be maintained so that the anodes keep their structural integrity after long durations of charge-discharge cycling. As stated earlier, increasing porosity of the anode can significantly reduce outer surface dendrite formation by consolidating many of the dendrites formed to be inside the pores of the anode. This will significantly increase the working capacity of the anode and also reduce shape change contributing to short circuiting.

It has been reported that cellulose can help introduce tunnels in the anode which can absorb electrolyte and hence reduce surface dendrite formation [19]. However, cellulose additive in the zinc anode researched in literature deal with anodes that are significantly thin. This is not

an ideal case especially in commercial applications. In commercial cells, one would want thicker zinc anodes to be used in order to maximize energy density in a single cell. Therefore, cellulose additive in zinc anodes will be investigated for thick anode designs.

The thesis' research work will also deal with ceramic anodes. Thick ceramic anodes will be fabricated, for which different pore forming agents will be experimented with and their effect on cell efficiency observed. The temperature treatment methods will be designed for simplicity and effectiveness so that the technique can be easily scaled for large scale anode fabrications. Ceramic anodes will have a definitive advantage over cellulose based anodes due to their high structural strength while also maintaining a high degree of porosity [40]. Both the ceramic and cellulose anodes will be alloyed with hydrogen evolution inhibitors.

3.2. Durable Nickel Cathode and Three Electrode Zinc Air Cell

Carbon gas diffusion electrodes for rechargeable zinc air batteries are not ideal. This is due to the fact that carbon tends to oxidize to carbon dioxide at high charging voltages. Therefore, a cathode needs to be designed which utilize a different support material. Nickel is an excellent support material due to the following reasons:

- High corrosion resistance in basic environments;
- High conductivity;
- Malleable allowing for extremely thin cathodes which are flexible and have good mechanical strength;
- Hydrophilic making them excellent support materials for the hydrophilic layer;

- During charging, they tend to oxidize to nickel oxide, which unlike carbon dioxide is a solid and stays in the cell;
- Nickel oxidized to nickel oxide can actually act as an OER catalyst in the cathode which can further improve performance; and,
- The cathode will not break down and leech into the electrolyte which is a major problem for carbon cathodes as demonstrated in Figure 13.

When designing the nickel cathodes, PTFE percentages need to be selected at both the hydrophilic and hydrophobic layer to get the perfect balance between porosity and flooding. Also, the fabrication technique needs to be kept as simple as possible to account for large area cathodes to be produced with minimal difficulty. These nickel cathodes will be excellent bi-functional cathodes for two electrode zinc air cells. This will ensure a high specific energy and volumetric energy density for each cell compared to a three electrode zinc air cell. However, the nickel based bi-functional electrodes can be expensive and in the case where specific energy and volumetric capacity is not an issue, a cheaper cathode needs to be designed for use in three electrode cells. A perfect example of practical application would be in grid energy storage, where compactness is not so much an issue. Therefore, a cheaper cathode for three electrode system will be fabricated and tested.

3.3. Zinc Air Packaging

Three different types of zinc air packaging will be designed for this research. The first generation of packaging will be designed for testing the fabricated anodes and cathodes. Its

design will be kept simple so that assembly is quick and parameters are kept consistent so that comparison of the different cathodes and anodes will be easier.

A large scale model of zinc air cells utilizing the bi-functional cathode will also be modelled. This design will account for the following:

- Maximum cathode area exposed to air and thin cells to increase specific and volumetric energy density;
- Efficient cell stacking to allow for ample air flow through the cathode surfaces;
- Tight sealing to prevent electrolyte leaking;
- Gas release valves to allow for hydrogen and oxygen escaping the tightly sealed cell; and,
- Allows for easy recycling via lids that can be opened to change out degraded anode and cathode.

The final zinc air cell design will be for a three electrode system that utilizes both an OER and ORR cathode. This will allow for cheaper ORR cathode and will reduce cost; however, the specific energy and volumetric energy density will be reduced. Anode degradation will be negligible as surface dendrite formation will be significantly reduced via use of a flow system to circulate electrolyte. This circulation of electrolyte minimizes uneven dendrite formation which is evident in non-flow cells as shown in Figure 4. Also, the ORR and OER cathode will be void of any degradation such as carbon leeching and flooding during charging. The flow setup will also ensure any buildup of pressure, due to generated oxygen and hydrogen in the cell, is released via circulation.

4. Characterization Techniques and Testing

Characterization techniques are really important in identifying certain properties of your prepared electrode. The imaging technique, scanning electron microscopy (SEM), will be used to analyze the cross-sectional and surface topography of the cellulose and ceramic anodes prepared. It will give one an idea of the pore sizes and their arrangement. Also, one can analyze dendrite formation before and after cycling using SEM.

The characterization techniques useful for the cathode will be BET surface area and porosity analyzer and contact angle. The BET will be mainly useful for identifying the porosity of the cathode. As the cathode is made from powders pressed together, it is important to know how much of the actual cathode volume will be made of pores. A pore volume of >50% is decent to get ample oxygen diffusion to the catalyst active sites without actually flooding the gas diffusion electrode with electrolyte. Contact angle values of the cathode surface will be useful to evaluate the degree of hydrophobicity of the cathode.

Finally, full cell testing will be conducted to get performance ratings of the cathode and anode. Some of the full cell tests include galvanodynamic current rate testing, accelerated cycling for degradation testing, and over-potential recording.

4.1. Scanning Electron Microscopy

Scanning electron microscopes were commercialized during the 1960s and they began to be widely used for characterization in various engineering and scientific applications. Their advantage over other simple microscopy techniques is the use of a high energy electron beam to probe the sample producing high resolution images. They produce a variety of signals, such as secondary electrons, backscattered electrons, x-rays, Auger electrons, photons, and sample current which can be used to characterize the specimen [41]. Schematic of an SEM is shown in Figure 15.

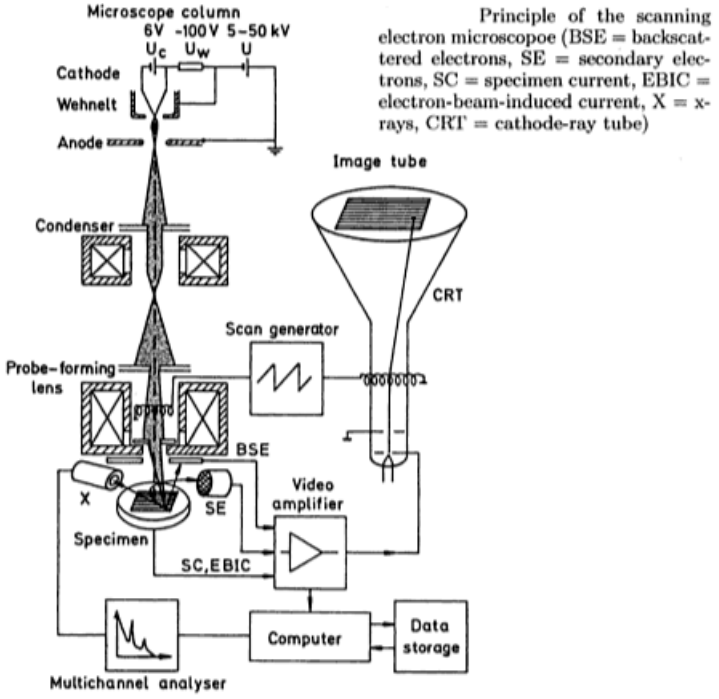

Principle of the scanning electron microscopoe (BSE = backscattered electrons, SE = secondary electrons, SC = specimen current, EBIC = electron-beam-induced current, X = x-rays, CRT = cathode-ray tube)

Figure 15. Schematic of SEM

Reproduced from [42] with permission of Springer Science and Business Media.

Electrons are emitted from a source, for example a tungsten tip, and these electrons are accelerated via a potential bias between the cathode and anode. These primary electrons are focused using electromagnetic lenses in a vacuum and the sample is probed by them in a raster. Secondary and back scattered electrons generated are captured by detectors and electrical signal output is produced. The computer processes this to create a 3D image of the surface probed. Secondary electrons will be utilized in this thesis' experiments to analyze the surface of the fabricated anodes to detect pore size and distribution as well as dendrite characteristic.

4.2. BET Analysis

The nickel cathodes fabricated will be analyzed using this technique. This analysis technique utilizes the phenomenon of gas adsorption. The inert gas that will be used for the adsorption is nitrogen. Nitrogen will adsorb on the outer surface of the cathode as well as the inner surface of the micro and meso-pores. This is normally evaluated at a reduced temperature of >77K which is maintained using liquid nitrogen. Prior to adsorption, the sample is prepared by heat treatment in vacuum to remove contaminant gas molecules. It is made sure that this pre-treatment temperature is kept below 300°C to prevent PTFE degradation in the cathode. The BET multilayer model will be utilized to determine parameters such as specific surface area and pore volume. Additional details of how this model works has already been discussed in Section 2.4.1.

The software included in the BET surface area and porosity analyzer machine will do the calculations from the raw data and provide one will the following important outputs:

- Specific surface area in m^2/g;
- Pore volume; and,
- Pore size distribution.

A schematic of a BET experiment setup is shown in Figure 16.

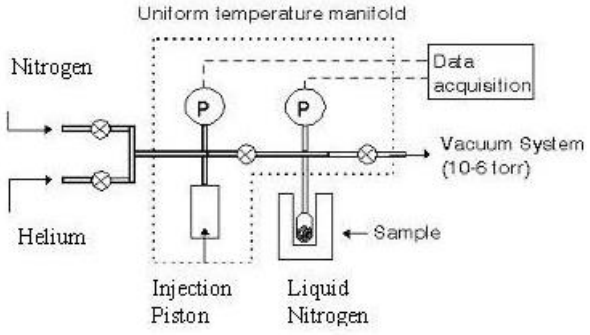

Figure 16. Schematic of BET [43]

4.3. Contact Angle Analyzer

Contact angles will be recorded for water droplets on the cathode surface. This will give the degree of hydrophobicity for the cathode. A drop shape analyzer will be used to measure the contact angle. A typical drop shape analyzer is shown in Figure 17.

Figure 17. Drop Shape Analyzer – DSA100R [44]

When taking measurements, it is important that the sample surface is as flat as possible and contaminants removed from the surface by air blowing. For measurement, basically the sample is mounted on the analyzer platform and a water droplet is dropped on the surface. A horizontal camera takes a perfect picture of the droplet and calculates the left and right angles between the droplet and cathode surface.

4.4. Full Cell Testing

Full cell testing will be conducted to get performance ratings of the cathode and anode. Some of the full cell tests include galvanodynamic charge and discharge, and galvanostatic cycling. As discussed earlier, test cell packaging were designed to house the anode and cathode. The design was such that assembly/disassembly of the cells would be simple and parameters

would be kept standard so that comparison between different anodes and cathodes would be easier. The schematic of the cell pieces is shown in Figure 18.

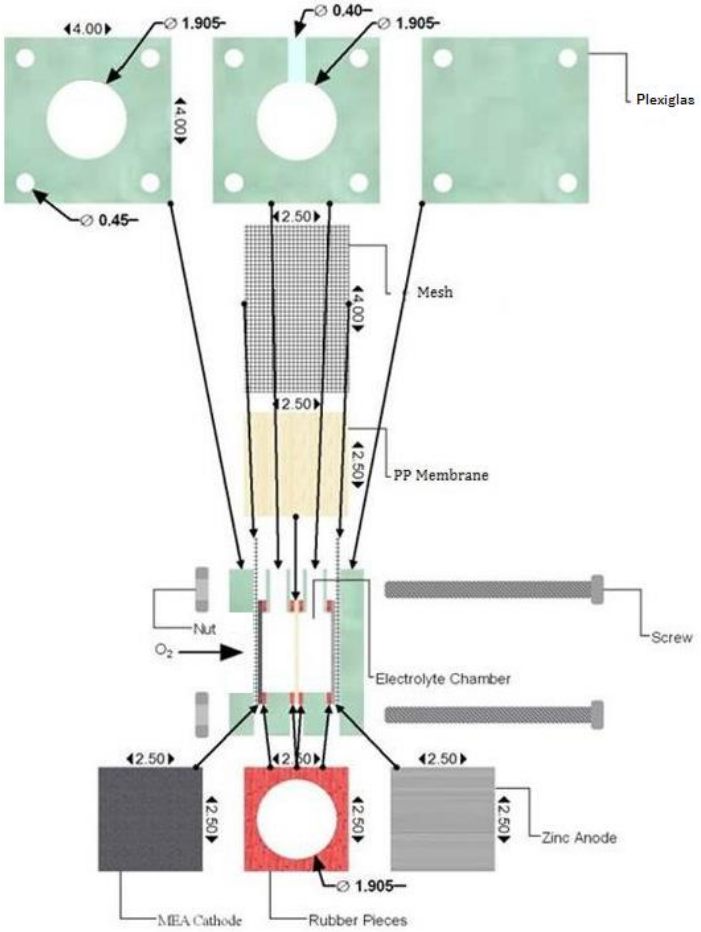

Figure 18. Testing Cell Schematic [45]

The packaging is made of polished Plexiglas which is a really good insulator as well as transparent. Therefore, it will be easier to monitor electrolyte level making sure to add water when the level drops due to drying. Four Plexiglas plates are used which are 0.5cm thick each. The center two plates have a hole drilled from the top to allow for gas escape and from which electrolyte will be filled and maintained. The gasket pieces are made of durable

silicone which is resistant to basic environments. The parts shown in the schematic are stacked against each other and sealed tightly using nylon screws and nuts.

The stack follows the specific order:

1. Plexiglas base with nylon screws attached.
2. Copper current collector.
3. Zinc anode.
4. Rubber gasket (anode side).
5. Plexiglas electrolyte chamber (anode side).
6. Celgard 5550 sandwiched between rubber gaskets.
7. Plexiglas electrolyte chamber (cathode side).
8. Rubber gasket (cathode side).
9. Gas diffusion electrode.
10. Plexiglas base with hole to expose cathode to air.

The dimensions of the parts are labelled in Figure 18 in centimeters. However, certain dimensions are subject to variations such as the air opening depending on the type of test. During all the tests it is made sure that the current is recorded in units of mA/cm^2 of cathode area. This will allow for fair comparison of all sizes of cathodes. A typical cell assembly is shown in Figure 19.

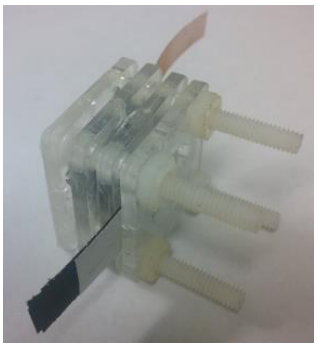

Figure 19. Typical Test Cell Assembly

All full cell tests will be conducted using a multichannel galvanostat/potentiostat. Using the machine, galvanodynamic and charge/discharge cycling tests will be run. Galvanodynamic testing will be especially important for the cathodes as it will give one the voltage profile for different currents. One would want the cells to generate a high voltage at a specific current.

Galvanostatic charge/discharge cycling will be conducted at a chosen current rating to monitor cathode and anode degradation. The change in over-potentials of the charge and discharge cycles will be closely monitored and drop in efficiency will be noted. All these durability tests will be accelerated, meaning the capacity utilized will be kept at ~1mAh/cm^2 to speed up the testing process. It is very important to note that a high capacity utilized would lead to greater degradation but for this research, the cycling will be accelerated and comparison of cathodes or anodes would be done at similar testing parameters.

When conducting tests for the fabricated anodes, a standard commercial gas diffusion electrode will be utilized. On the other hand when testing the fabricated cathodes, a standard bulk zinc plate will be used. This is to standardize and simplify the opposing electrode when analyzing either the anode or cathode. The commercial gas diffusion electrode lacks the

catalyst in the hydrophilic layer. Therefore, spraying technique will be utilized to incorporate the catalyst on the commercial cathode surface. The commercial cathode used is a 350µm thick soft puffy carbon gas diffusion electrode. SIGRACET® Gas Diffusion Media, Type GDL 35BC is used. Steps to prepare the catalyst/GDE assembly are listed as follows [46]:

- Catalyst preparation: Clean the spatula with ethanol or isopropyl alcohol. Use it to transfer 15mg of cobalt (II, III) oxide nano-powder on to a weighing paper. Transfer the measured cobalt oxide to a 7mL vial. Add 1.532 ml of isopropyl alcohol to the cobalt oxide. Sonicate the solution for 35 minutes. Add 102.6µL of 5wt% nafion to the solution (34.2µL for 15wt%). Sonicate the solution for another 30 minutes.

- Gas Diffusion Layer (GDL): Cut GDE papers off SIGRACET® Gas Diffusion Media, Type GDL 35BC using gasket punch cutters of size 1.3125’’. Weigh the GDE paper and take note of its mass.

- Spraying Process: The spraying process takes place inside the fume hood. Before starting to spray, ensure that the spraying gun is submerged inside isopropyl alcohol for a minimum of 30 minutes. Secure the GDE paper on a piece of cardboard to facilitate the spraying process. Fill up the guns reservoir with isopropyl alcohol and spray out the alcohol to ensure that all internal components of the gun are rinsed out. Fill up the reservoir with the catalyst solution that was prepared earlier. Start spraying away on the paper from up to down and left to right making sure the catalyst layer deposited has a consistent thickness throughout. Make sure that the wet catalyst ink is allowed to properly dry during the spraying session. Remove the GDE paper and

place inside an aluminum dish and cover it with aluminum foil. Put the dish inside a 60°C oven to fully dry out. Finally weigh the GDE paper to get the difference between the before and after masses. This will give the mass of catalyst with nafion deposited on the GDE and one can estimate the yield. The yield loss should be no more than 6mg to get a decent cathode performance.

5. Effect of Cellulose Additive in Thick Zinc Anodes

Cellulose additive in zinc anodes have a tendency to absorb electrolyte, thereby increasing the overall inner surface area of the zinc. This is really important in reducing surface dendrite formation and increasing the working capacity. Research will be conducted in seeing the how the percentage of cellulose added will affect the overall capacity of the anode and certain conclusions will be made from acquired results.

5.1. Experimental Method

The chosen anode size and thickness are 6.41cm^2 and 2.5mm respectively. For a defined size, the total mass of solid mixture required is ~2.365g and this has been calculated by taking into account average bulk particle density. The solid mixture slurry is made of 90wt% ZnO, 5wt% PTFE, 5wt% cellulose, and 10mL isopropanol per gram of solid. ZnO is used instead of Zn because Zn does not tend to disperse evenly in the slurry and therefore, it is impossible to make a dough-like material. ZnO will be used which gives an excellent consistency in the mixture and the anode will later be fully charged to change most of the ZnO to Zn. The flowchart summarizing the experimental steps is shown in Figure 20.

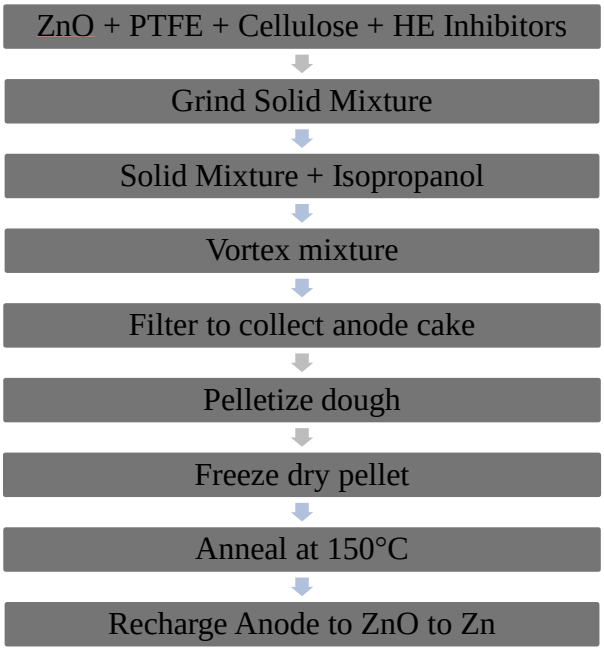

Figure 20. Thick Cellulose Anode Fabrication Flowchart

1000ppm of indium and bismuth are added which will act as hydrogen evolution inhibitors. Any less than 600ppm will lead to noticeable hydrogen evolution and this has been experimentally tested in the lab. When adding PTFE to the slurry, it is made sure that the PTFE 60wt% emulsion in water is added in a drop-wise fashion to the slurry, stirring all the while. Stirring is done for 1h. The slurry is then filtered to collect a dough-like material which is rolled and pelletized using a mechanical press in a mold of size 6.41cm^2. The pressure applied is 1500psi and this is maintained for 5min. The pellet is quickly transferred to a beaker cooled with liquid nitrogen and then transferred to a freeze drying chamber for 12h. This is to prevent the thick anode from breaking. Finally, the pellet is annealed at 110°C for 1h. The anode fabricated is shown in Figure 21.

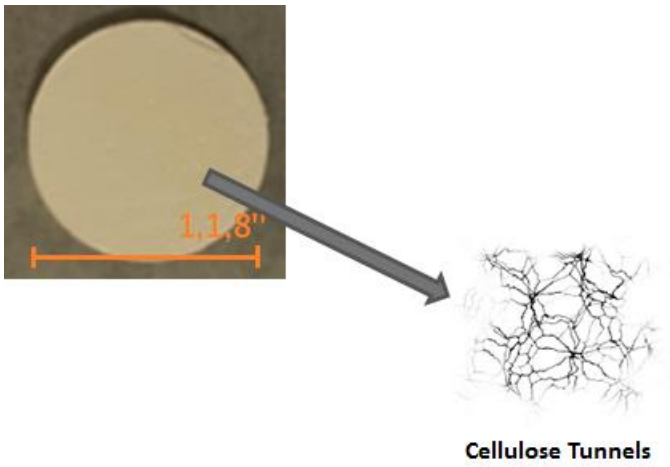

Figure 21. Thick Cellulose Anode [47]

Three different specimens are fabricated: with 1wt%, 5wt%, and 10wt% cellulose. The weight percentages are traded between ZnO and cellulose; e.g. 94wt% ZnO with 1wt% cellulose.

5.2. Results and Discussion

The anodes fabricated were then analyzed using SEM. This will give the surface topography of the anode. All the anodes had similar topographical image because they are fabricated the same way. The SEM image of the anode with 5wt% cellulose is shown in Figure 22.

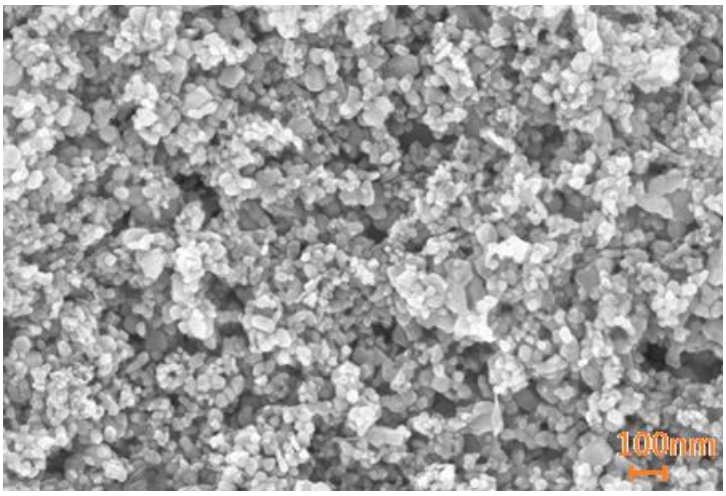

Figure 22. SEM Image of Cellulose Anode

The anode looks mesoporous in nature with pores ranging between 10-100nm. However, the actual inner surface area will be greater than apparent because the hygroscopic cellulose solid particles will absorb the electrolyte. This will expose more of the Zn/ZnO to the electrolyte. The anodes were charged for 450mAh and then discharged to see the effect of cellulose on the capacity efficiency. The discharge curves are shown in Figure 23.

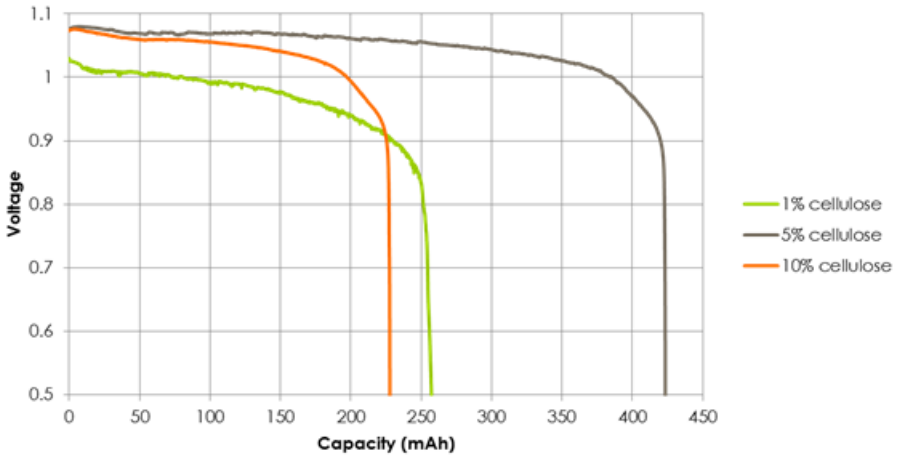

Figure 23. Thick Cellulose Anodes Discharge Curves

The anodes were discharged using a current of 10mA/cm^2 of cathode area. From the graph, the following capacity efficiencies can be calculated:

- 1wt% cellulose: 58%;
- 5wt% cellulose: 94%; and,
- 10wt% cellulose: 52%.

Increasing cellulose shows a significant increase in cell voltage (from 1V to 1.1V) which proves the improved wetting of anode by the electrolyte. However, the working capacities do not follow such a trend. 5wt% cellulose gives a massive increase in working capacity proving the benefits of cellulose. However, 10wt% cellulose shows a drop in efficiency. After analyzing the post discharge anode for the 10wt% cellulose, one can see that the anode has cracks and has broken into pieces. This is because of the changing characteristic of cellulose when it absorbs the electrolyte. When cellulose absorbs water, it expands to twice its size. Therefore, increasing the cellulose content in the anode will lead to anode expansion and contraction during the charge/discharge cycling. A perfect balance needs to be maintained in the amount of cellulose so that there is enough wetting without causing a detrimental effect to the structural integrity. Thus, one can see the efficiency loss in the case of 10wt% cellulose due to pieces of the anode breaking apart and losing contact with the conductive anode network rendering them non-dischargeable.

Even though 5wt% cellulose may be the optimal percentage of additive, the idea of cellulose expansion and contraction contradicts its solution of preventing dendrite formation. The reason behind preventing dendrite formation is the fact that over time through charge and discharge cycling, the dendrites eventually lead to shape change which can ultimately lead to

loss of capacity and short circuiting. Cellulose additive has the benefit of greatly reducing this dendrite formation but it itself contributes to the very shape change it is trying to prevent via constant expansion/contraction. This stress on the anode will eventually lead to shape change and loss of efficiency and therefore, cellulose is the not the ultimate solution as many of the papers in literature state.

6. Additive Investigation in Thick Ceramic Anodes

The advantage of ceramic anodes over cellulose anodes is the high mechanical strength. This is not compromised when the porosity of the anode is increased. This mechanical strength is analogous to commercial ceramic materials as the method of fabrication is very similar to how ceramic materials are made in the industry. However, the complex heat treatment process makes anode fabrication difficult and long; therefore, it is ideal only for industrial use where large batches of anodes are fabricated together in huge furnaces.

The mechanism of micellar formation will be utilized to create pores in the ceramic. This is a very unique method which makes use of surface energy and molecular interaction between the molecules to create a certain pore distribution. The major pore forming additive is a non-polar solvent with a vapor density lower than that of water. A measured quantity of surfactants are added which will allow for the non-polar solvent to disperse evenly in the slurry as micelles. Over time as the slurry hardens, the non-polar solvent will evaporate leaving pores in its place. The schematic of the slurry is shown in Figure 24.

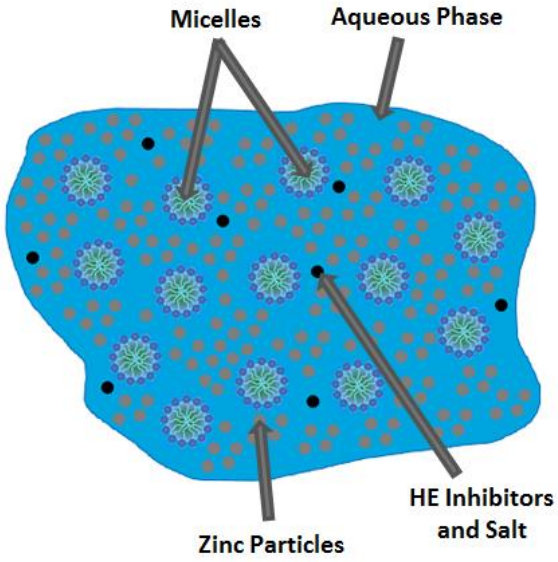

Figure 24. Schematic of Pore Forming Mechanism in Ceramic Anodes

The grey particles are the zinc particles and the black particles are the hydrogen evolution inhibitors and salt. These hydrophilic particles are dispersed in water using carboxymethyl cellulose as a binder. This binder makes the slurry viscous; therefore, preventing settling of the heavy metal particles. The binder will later be burned away in the furnace which will create further macropores in the ceramic. The micelles shown are created by the non-polar solvent which is surrounded by surfactants.

6.1. Experimental Method

Zinc is used in the formation of the slurry as it is not as dilute as the one prepared for the cellulose anode. As usual, the hydrogen evolution inhibitors, indium and bismuth, are added in 1000ppm to the zinc powder. 1% by volume salt is also added which will later be dissolved

away to introduce macropores. The particle sizes for the powder are chosen to be <1μm so that the slurry dispersion is consistent. The zinc mix is added to water such that the zinc mix to water volume ratio is 9:11. To this mixture, 0.15% by volume sodium lauryl sulfate (SDS) and 5% by volume carboxymethyl cellulose (CMC) is added. The amount of SDS is very important as it will determine the pore size and distribution in the ceramic anode. Finally, add the non-polar solvent in excess to the mixture. This will create the micelles in the slurry dispersion which will be surrounded by SDS. The size of the micelles is determined by the type of non-polar solvent and the amount of micelles by the quantity of SDS. The excess non-polar solvent which does not take part in the micellar formation will float on top of the slurry dispersion which can be poured away. The flowchart in Figure 25 summarizes the preparation of the slurry.

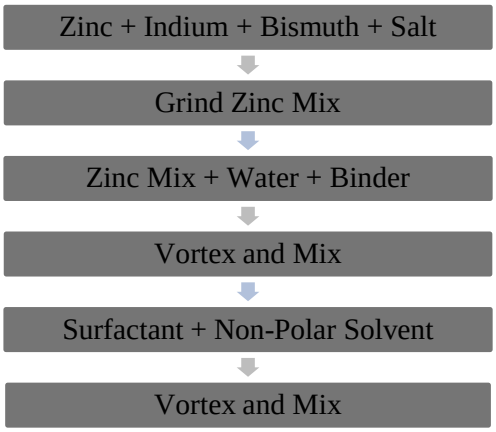

Figure 25. Ceramic Anode Slurry Preparation Flowchart

This slurry is scooped and filled into premade Pt/Si molds of size 6.41cm^2 and 2.5mm deep indentation. This is shown in Figure 26. This is allowed to dry on a 24h period. During the drying process, several mechanisms occur in the slurry. The water mixture hardens forming a

solid structure. At the same time, the non-polar solvent in the micelles evaporate leaving porous voids in the solid matrix. The solid anode is still weak in structural strength and care needs to be taken when handling them at this step.

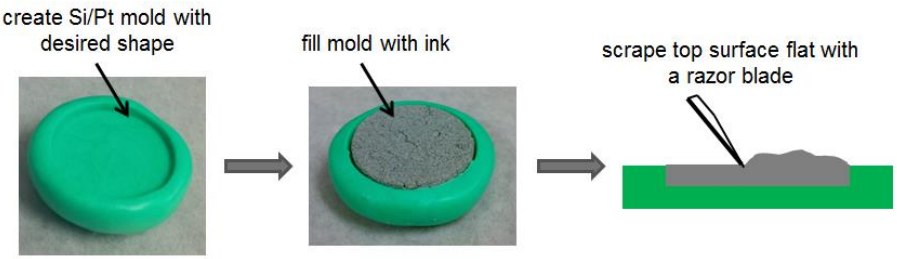

Figure 26. Ceramic Slurry Drying in Mold

The prepared solid anodes are sandwiched between smooth marble plates which are transferred to a furnace. The marble plates will prevent the anode from bending during the heat treatment process. The schematic of the furnace setup is shown in Figure 27. The electrode is first heated in argon from room temperature to 400°C at 5°C/min and kept sintering at this temperature for 1h. This step ensures that the particles stick to each other. It is then raised above 420°C (the melting point of zinc) but well below the melting point of ZnO at 5°C/min in presence of air to form a hard oxide shell. The zinc oxide shell forms on the surface exposed to air. This includes the outer surface as well as the inner surface of all the pores. The metal zinc melts and fuses together to form a continuous conductive network inside the zinc oxide shells. This fusing process occurs for 1h. Any polymer material will fully carbonize and burn away during the annealing process. The anode is then cooled to room temperature and extracted from the marble plates. This anode is soaked in water to dissolve the salt away forming further macropores. Before full cell testing, the anodes are pre-charged (observable H_2 evolution denotes an almost fully reduced anode).

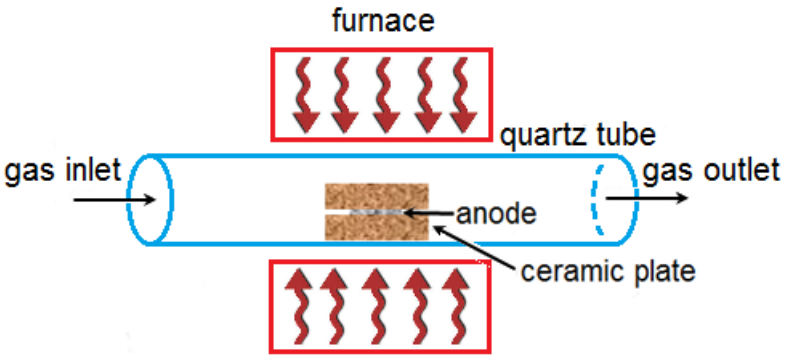

Figure 27. Schematic of Furnace Setup for Ceramic Anode

6.2. Results and Discussion

The final ceramic anode is shown in Figure 28. The product is a zinc network that is continuous and conductive, and there are pores distributed throughout that are lined by a thin layer of zinc oxide. The SEM images of pre-annealed and annealed anodes were taken to see the effect of heat treatment on the surface topography. These SEM images are shown in Figure 29 side by side for comparison. The left images show the pre-annealed surface, whereas the right shows the surface after the complex heat treatment. It can be seen for the pre-annealed images that the electrode is only slightly porous but the zinc is not a continuous network. Also, the surface is smooth due to presence of binder and has no zinc oxide layer. For the annealed anode, one can see circular voids formed by the micelles. Also, the zinc has a continuous structure with spikes of zinc oxide covered throughout which have a size of ~5μm. At highest magnification which is more evident in Figure 34, one can see the tiny pores which are a result of polymer carbonization and burning, and salt dissolution.

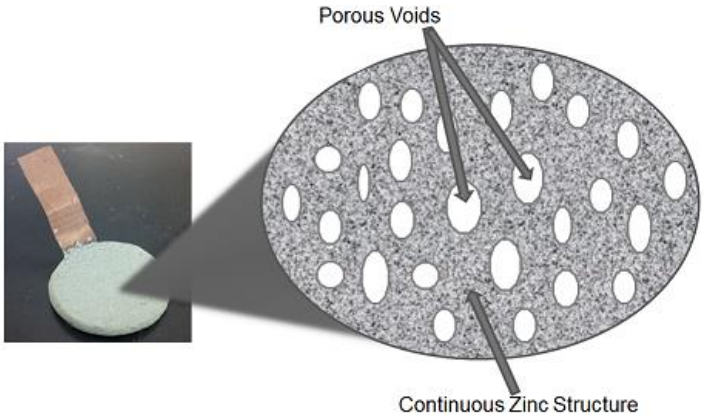

Figure 28. Ceramic Zinc/Zinc Oxide Anode with Copper Mesh

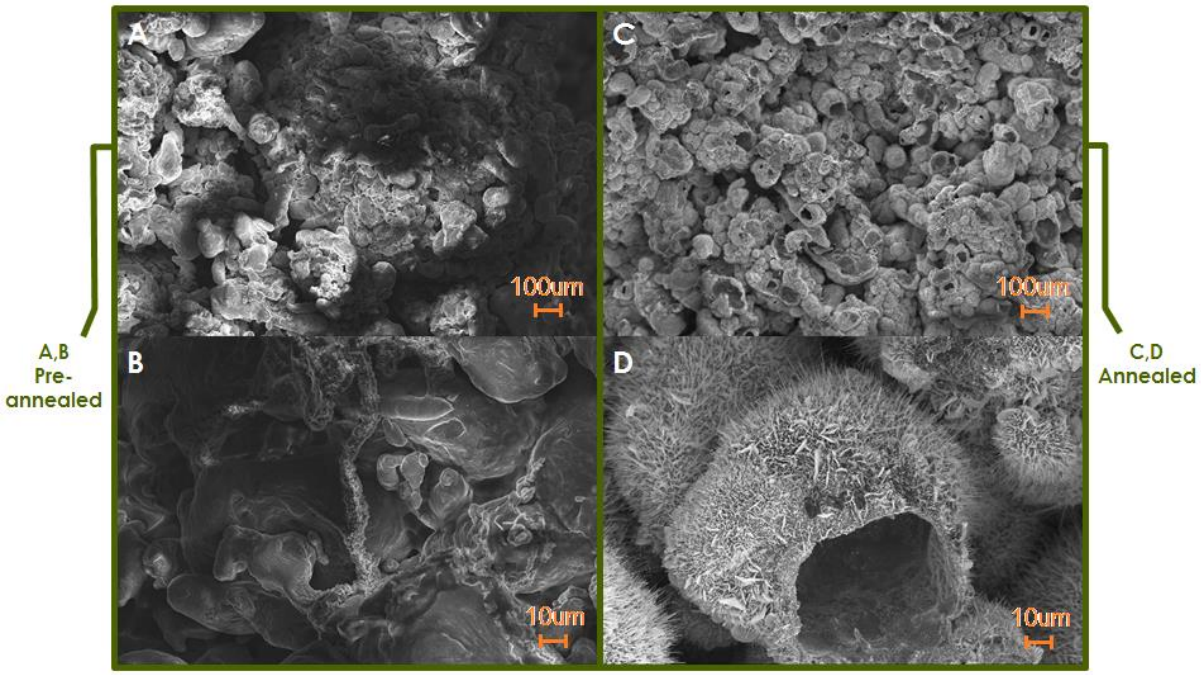

Figure 29. SEM Images of Ceramic Anode (Pre-annealed and Annealed)

Two different anodes were fabricated; the difference between the two being that one utilized dodecane whereas the other ultilized decane for micellar formation. Dodecane and decane have vapor pressures of 18Pa and 195Pa respectively. This will determine how the micellar voids were created as both of them have different evaporation rates but very similar

structures. From the charge/discharge cycling curves shown in Figure 30, the improvement in performance from use of ceramic anodes is evident. Full cell cycling tests were conducted for the three different anodes: bulk zinc plate, ceramic anode made using dodecane, and one using decane. Conditions were 10mA/cm^2 of cathode area and 5min C/D cycling.

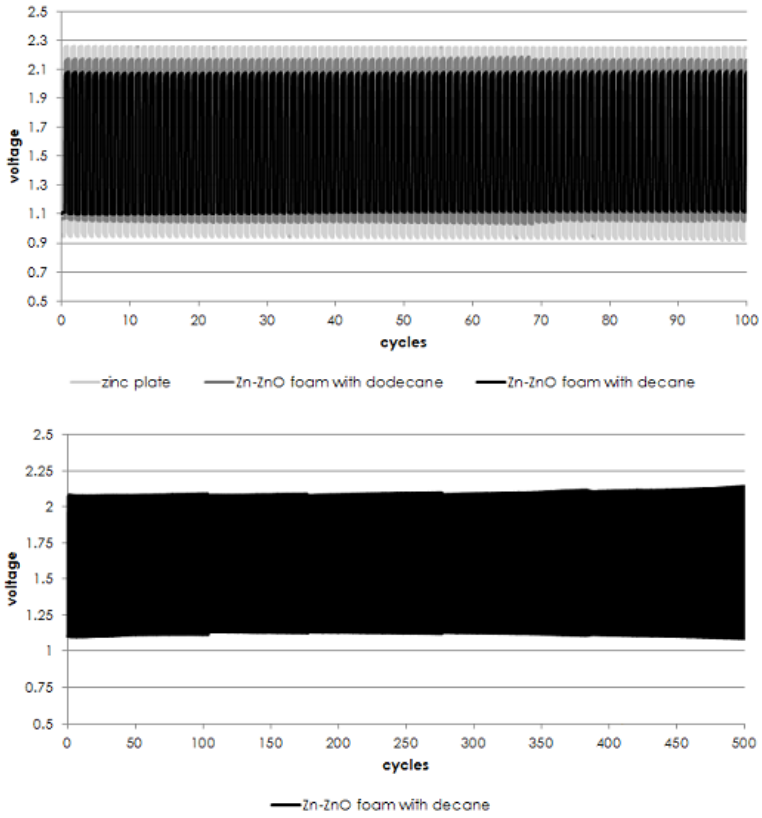

Figure 30. Ceramic Anodes Galvanostatic C/D Curves

The cycling curves for the ceramic anodes show a significant improvement in the over-potentials for both charge and discharge. This is due to an increase in overall porosity of the anode leading to greater electrolyte wetting, and reduction in hydrogen evolution. Not only that, dendrite formation was significantly reduced and this is evident from the images shown in Figure 31, where the ceramic anode had reduced shape change at the bottom of the anode.

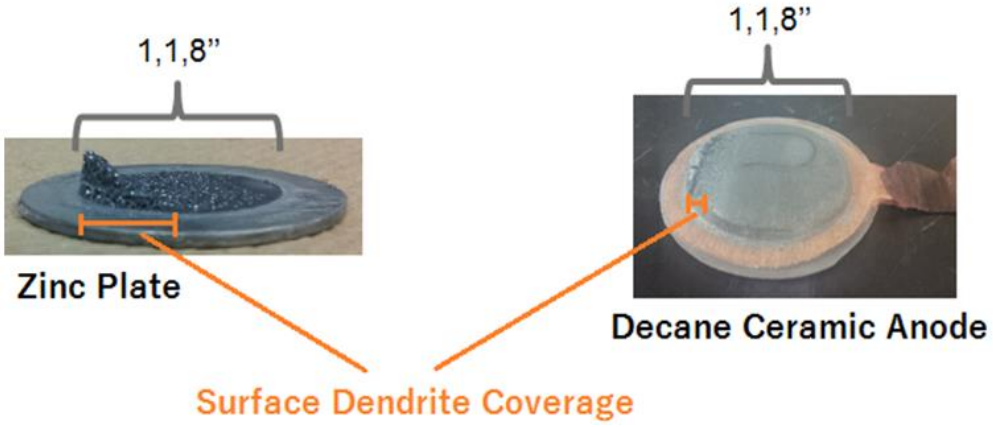

Figure 31. Dendrite Formation after 100 Cycles

There is also a slight difference in over-potentials for the dodecane and decane anodes. This is because of smaller number of pores for the dodecane based anode. Dodecane has a lower vapor pressure compared to decane; therefore, it evaporates slower during the drying process. When the water based slurry fully hardens, most of the water has evaporated due to it having a higher vapor pressure (3.17kPa). Dodecane has a very low vapor pressure which stays in the hardened base. As hardly any water is present, the micelles disintegrate at locations which are dry. Therefore, it is very important for the non-polar and polar solvents to evaporate simultaneously but with one having a slightly lower vapor pressure than the other. Too large a difference in vapor pressure can destroy the micellar voids.

The superior anode, which is the decane one, was cycled for longer. As can be seen in Figure 30, the over-potentials after 500 cycles have hardly increased which clearly shows the high durability of the anode. Exact over-potentials for the anode was extracted in absence of the commercial cathode (major contributor to over-potential) using the cell setup shown in Figure 32. A platinum wire as the counter electrode and a bulk zinc plate as the reference electrode were utilized. The platinum wire was at the center of the cell separated from the other

electrodes with Celgard 5550 membranes and the cathode was replaced by the bulk zinc plate. The over-potential curves for difference current densities are shown in Figure 33.

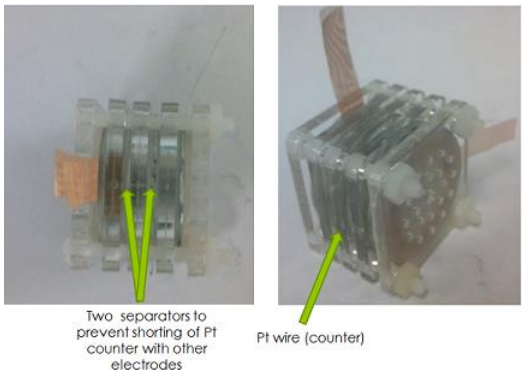

Figure 32. Half Cell Setup for Ceramic Anode

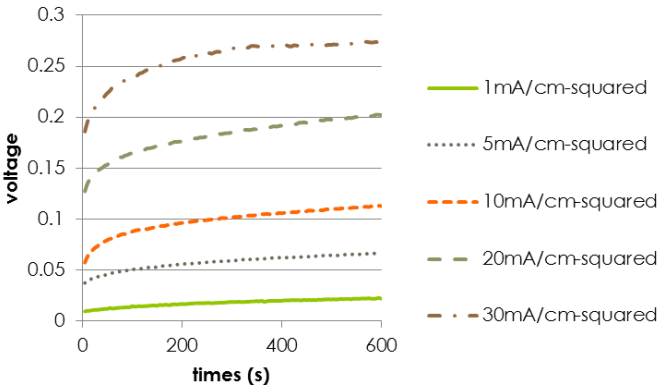

Figure 33. Over-potentials of the Ceramic Anode

SEM images were also taken for the decane based ceramic anodes post-cycling. During sample preparation for the post-cycling anode, the sample was gold sputtered at the cross-section to create a conductive coating on the surface. This is because there is a greater degree of non-conductive ZnO on the surface preventing finer details of the surface from being analyzed by the SEM. The differences in topography can be evaluated from the pre and post-

cycling detailed SEM images included in Figure 34 and 35. One does not see much change in the post-cycling images; however, the surface area of the electrode is covered with crustier zinc-oxide formations if observed closely. The dendrites are in the same order of magnitude being in the range of 1-10µm. This clearly shows the superiority of the anode as there is no sign of anode breakage or shape change.

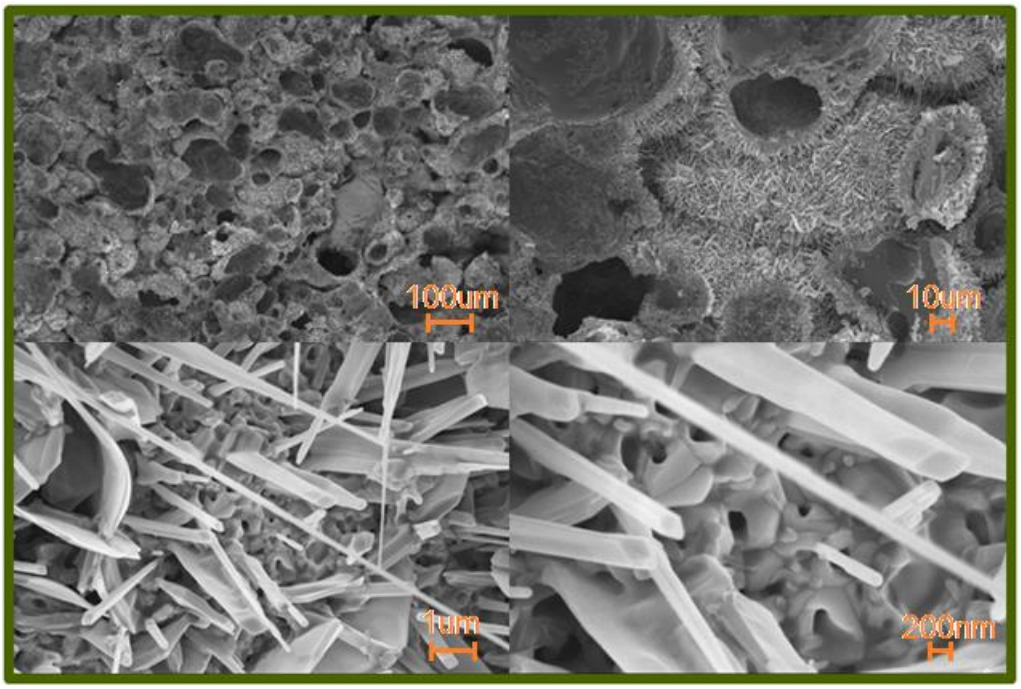

Figure 34. SEM Images of Ceramic Anode (Pre-cycling)

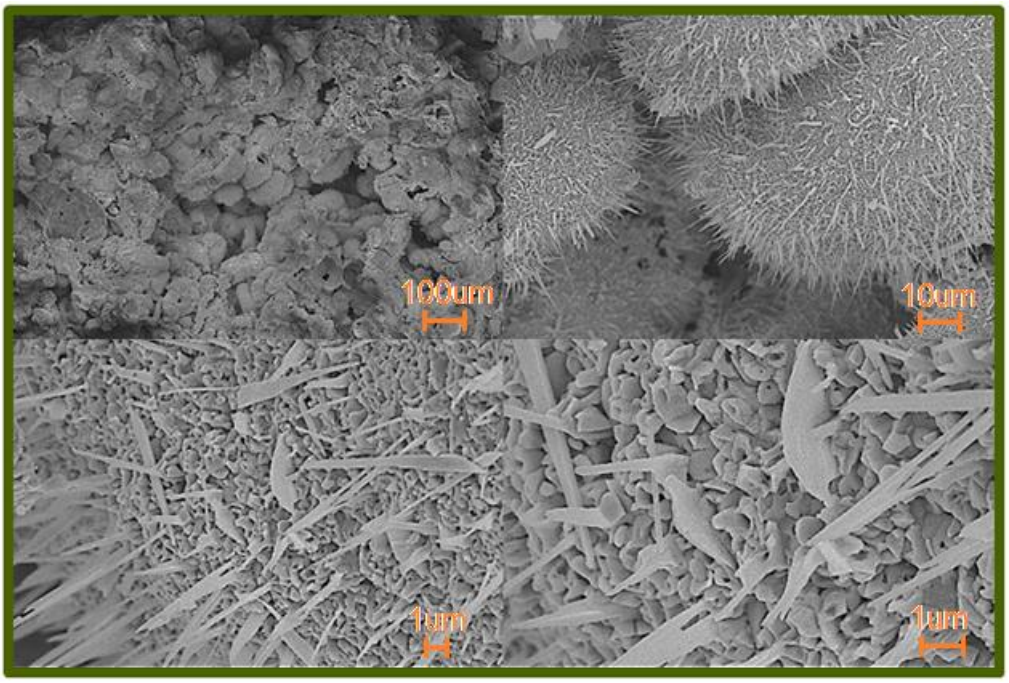

Figure 35. SEM Images of Ceramic Anode (Post-cycling)

Therefore, one can conclude that thick ceramic anodes can be used in zinc air batteries by modifying the structure using the above mentioned technique. Using these anodes, one will be able to greatly increase the energy density of the cell, decrease surface dendrite formation, and increase lifetime. It is important to note that dendrite formation can be further reduced by utilizing a cell that has a flow system. Preliminary experiments will be done using the flow system in one of the following sections.

Also, from Figure 33, it is evident that the over-potential contribution from the zinc anode is very low (only 0.11V at 10mA/cm^2). For a full cell test, the anode gave an overall voltage of 1.1V. This is a total over-potential of 0.38V as the open circuit voltage of the cell is 1.48V. The anode contribution to the over-potential is only 0.11V, whereas the rest coming from the

cathode. This shows that the majority of the efficiency loss is coming from the cathode side making it more vital to optimize it.

7. Nickel Gas Diffusion Electrodes Made via Mechanical Press

As discussed earlier, the gas diffusion electrode needs to consist of three layers: current collector, hydrophilic layer, and hydrophobic layer. 20wt% PTFE, being the ideal composition for a carbon gas diffusion electrode, will be used as the basis for the nickel cathode layer designs. A 20wt% PTFE in a carbon gas diffusion electrode is equivalent to 20vol%. This is because of similar densities between PTFE and carbon. In order to keep the molecular ratios approximately similar for the nickel based cathode, one would need to work with volume ratios. This will take into account the heavier density of nickel in the design of the cathodes. 20vol% PTFE in a nickel based cathode is equivalent to 5wt% PTFE. This makes sense given the fact that Ni has almost 4 times the density of acetylene black.

7.1. Experimental Method

15vol% PTFE will be used for the hydrophilic layer. This is to ensure the layer is sufficiently wetted by the electrolyte. The hydrophobic side, on the other hand, will have 20vol% PTFE. This is to ensure that there is decent porosity without compromising the hydrophobicity of the layer as the main function of this layer is to adsorb oxygen and prevent electrolyte flooding. Thus, the hydrophobic layer will comprise only of Ni and PTFE. However, the hydrophilic layer will have four major components in the design and this is shown in Figure 36.

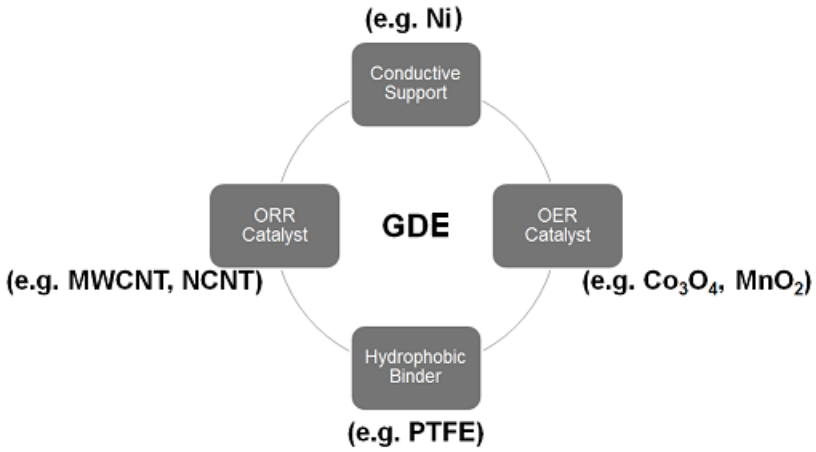

Figure 36. Schematic of GDE Composition

15vol% PTFE will be utilized as stated earlier. 20vol% Co_3O_4 and 15vol% MWCNT will be used as a composite catalyst. Co_3O_4-MWCNT is an excellent bi-functional composite catalyst that is highly durable and relatively cheap compared to noble catalysts. The catalyst quantities are obviously in excess so that the catalyst amount is not the limiting factor in the performance of the cathodes. By calculating the average density of the mixture from the bulk densities of each particle, one can approximately find the total amount of solid required to make a GDE of a certain area and thickness. The thickness of the hydrophilic layer is chosen to be 350µm thick whereas the hydrophobic layer as 200µm.

The GDEs are made following the steps shown in the flowchart in Figure 37. When making the hydrophilic and hydrophobic layer slurries, excess isopropanol is used. The doughs acquired after filtration are kneadable to a desired shape. The hydrophobic dough is sandwiched with a Ni screen of mesh# 200 and mechanically pressed at 1000psi in a mold of the desired area. The hydrophilic dough is then stacked on top of the hydrophobic layer and

pressed again to create the three layered GDE. The GDE is finally annealed between 300°C to 340°C for 0.5h which sinters the PTFE binder and enhances its hydrophobic properties.

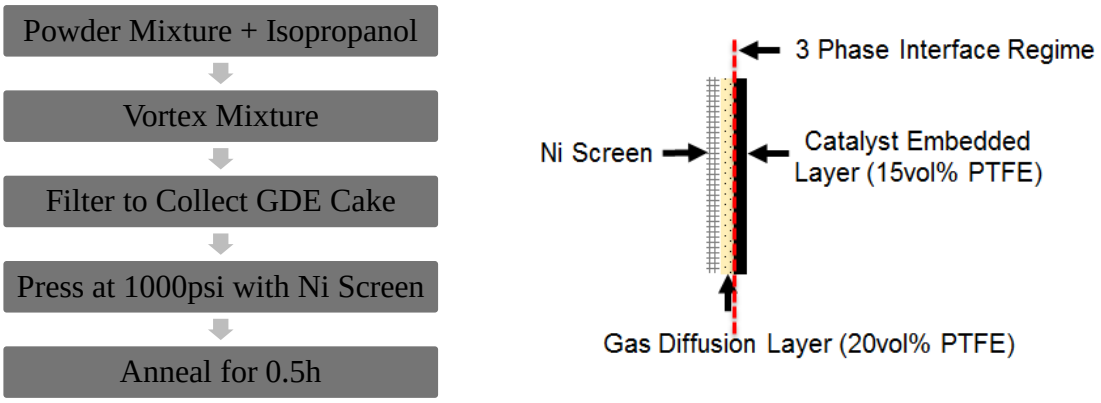

Figure 37. GDE Fabrication via Mechanical Press Flowchart

7.2. Results and Discussion

In Figure 38, a typical mechanically pressed three layered GDE is shown. This GDE was assembled in a full cell against bulk zinc plate and cycled at 10mA/cm^2 with 5min C/D cycling for 100 cycles (Figure 39). A discharge voltage of 1.1V was achieved which is significantly higher compared to that of the commercial GDE vs. zinc plate shown in Figure 30.

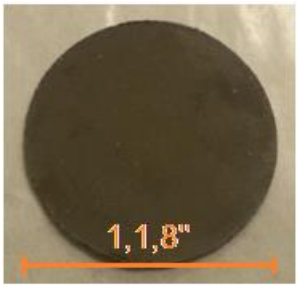

Figure 38. Nickel GDE Fabricated via Mechanical Press [48]

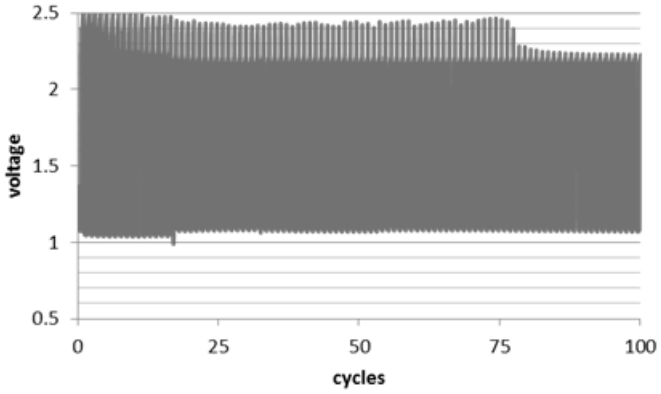

Figure 39. Nickel GDE Fabricated via Mechanical Press C/D Cycles

A high initial charge voltage is observed which later stabilizes to 2.15V. The spike in charge voltage occurs right at the end of the cycle and this is due to the lack of zincate species rather GDE limitation. Therefore in future tests, 0.2M zincate species (using zinc acetate) will be dissolved in the electrolyte. This will act as the reservoir of zinc oxide for charging as the bulk zinc plate lacks presence of any significant zinc oxide unlike ceramic anodes. Even though voltage efficiencies were significantly improved and carbon corrosion was fully eliminated, the hydrophobic layer of the Ni based GDE eventually shows signs of electrolyte leakage as shown in Figure 40.

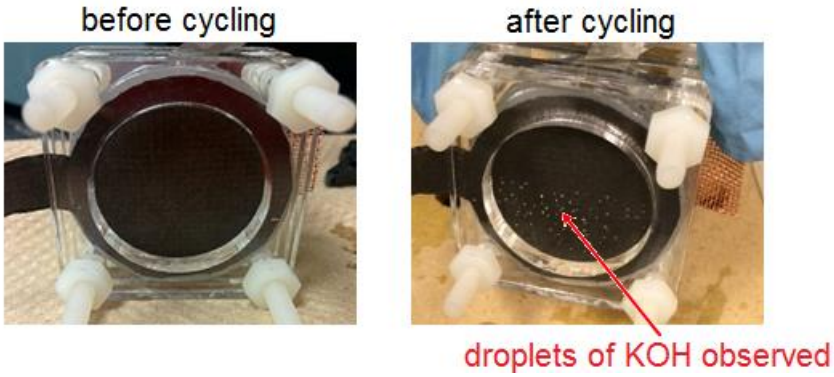

Figure 40. Nickel GDE Electrolyte Leakage after 100 Cycles

This is more due to the hydrophilic characteristic of Ni rather than porosity. The only way to prevent this is to fully eliminate any hydrophilic materials from the back layer of the gas diffusion electrode. This will be address in the following section where a PTFE only super hydrophobic PTFE only gas diffusion layer will be utilized. Not only that, porosity of the hydrophilic layer will be further improved via use of a new fabrication technique.

8. Nickel Gas Diffusion Electrodes Made via Roll Press

The new Ni gas diffusion electrodes will use a PTFE only hydrophobic layer. The PTFE only hydrophobic layer will be made from PTFE filtration papers. These PTFE films can be purchased online. A membrane that is 70% porous by volume and 200µm thick will be utilized. The GDE stack will be prepared using a roll press. Fixed width rollers have the advantage of fine control of GDE thickness without excessively compressing the GDE. This will ensure sufficient porosity in the electrode. Not only that, large area electrodes can be prepared using this technique which is beneficial in an industrial application. The GDEs fabricated will consist of the three layers: nickel screen current collector, 350µm thick hydrophilic layer (50vol% Ni, 20vol% Co3O4, 15vol% MWCNT, 15vol% PTFE), and 200µm thick PTFE film.

8.1. Experimental Method

The fabrication procedure is simplified in Figure 41. Three different layer orientations were investigated. These are shown in Figure 42.

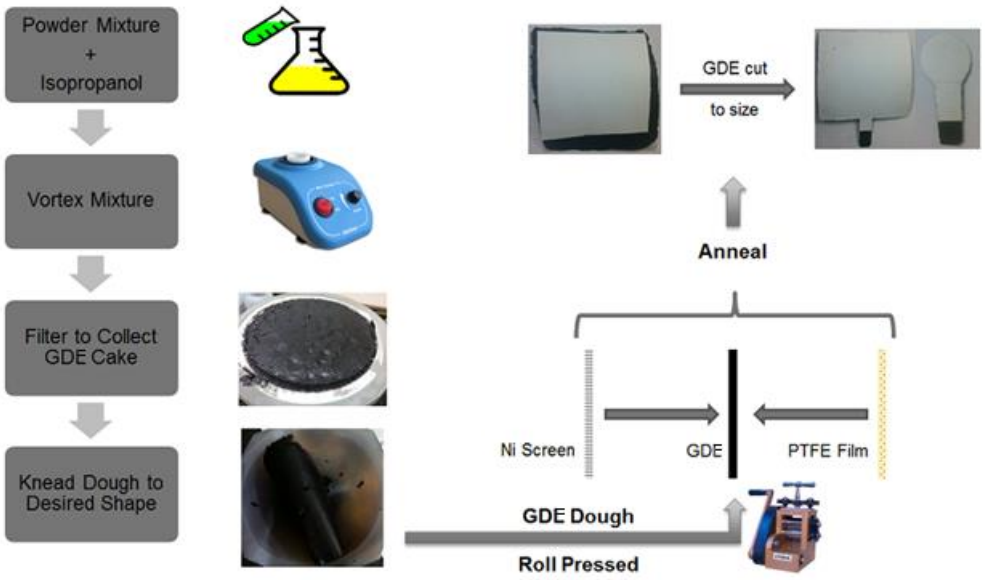

Figure 41. GDE Fabrication via Roll Press Flowchart

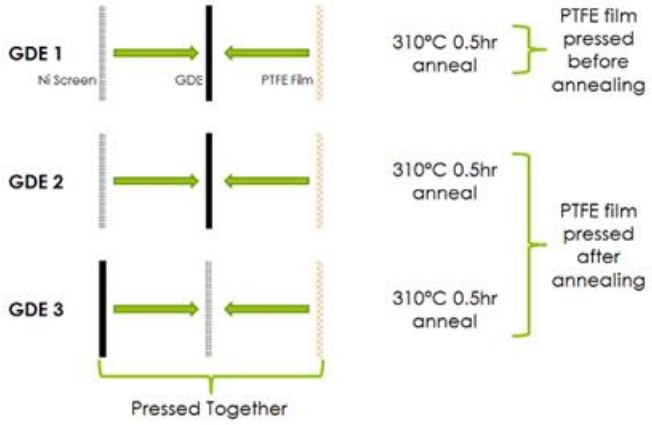

Figure 42. GDE Layer Stack Orientations Investigated

8.2. Results and Discussion

The GDEs of the orientations in Figure 42 were assembled into full cells and cycled for 100 C/D cycles. Conditions were 30min/cycle (1 cycle includes 1 C and D), 10mA/cm^2 current

density, and 6M KOH with 0.2M zinc acetate. In intervals of 0th cycle, 25th cycle, and 100th cycle, galvanodynamic discharge results were obtained and these are shown in Figure 43.

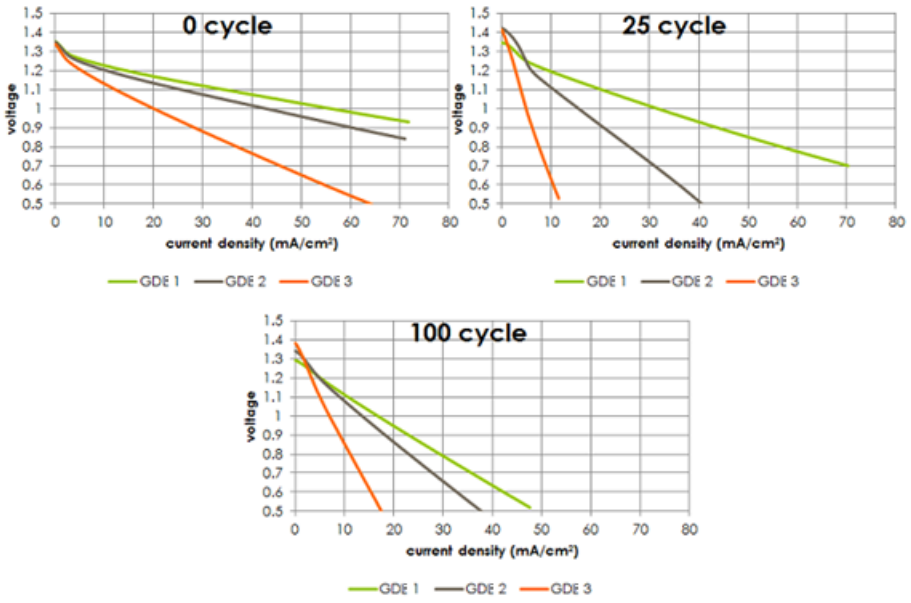

Figure 43. Galvanodynamic Discharge Curves for 3 Differently Stacked Ni GDEs

It can be concluded from the results that annealing the PTFE film along with the hydrophilic catalyst layer, ensures sintering of the two and creating an optimal 3 phase interface regime between the two where oxygen, catalyst, and electrolyte meets for the reaction. Thus, one can see the performance superiority of GDE 1 over GDE 2. On the other hand, GDE 3 is an unsuitable design as the high voltage bias experienced at the Ni screen creates the electro-osmosis phenomenon discussed earlier which absorbs the electrolyte between the catalyst layer and PTFE film destroying the 3 phase interface regime. The reduction in rate performance over-time for the electrodes is due to the loss of 3 phase interface regime sites in the electrode. Initially the hydrophilic layer is partially hydrophobic; therefore, containing many 3 phase interface regimes sites in it. Over-time, the hydrophilic Ni support absorbs all

the electrolyte limiting the 3 phase interface regime to only the thin separation between the hydrophilic layer and PTFE film. 10mA/cm^2 is the ideal current density which does not experience this vast change in voltage. This is further confirmed by cycling a new GDE 1 at 10mA/cm^2 at 5min C/D cycling for 500 cycles continuously. The cycles are shown in Figure 44 where minimal over-potential change is observed.

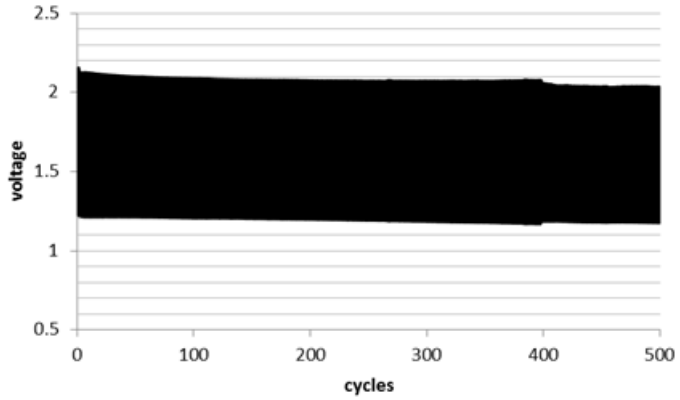

Figure 44. Nickel GDE Fabricated via Roll Press C/D Cycles

BET analysis was conducted on GDE 1 to analyze specific surface area, pore distribution and volume, and total volume % of pores. The PTFE film was peeled off to study the Ni based hydrophilic layer. The curves produced are shown in Figure 45. The software does the calculations from the BET isotherm produced and gives the value of surface area. The BET surface area of the GDE is 184.425m^2/g. The adsorption cumulative pore volume is 0.182cm^3/g. Given that the average real density of the GDE is 3.857g/cm^3, the pore volume is calculated to be 70%. The pore distribution curve shows diameters ranging between 0-120nm. This is decent given that the average particle size of the Ni GDE is 32.534nm. The log differential adsorption is important to locate where the majority of pores are clustered in. It is clearly obvious that most of the pores fall in the ~10nm range.

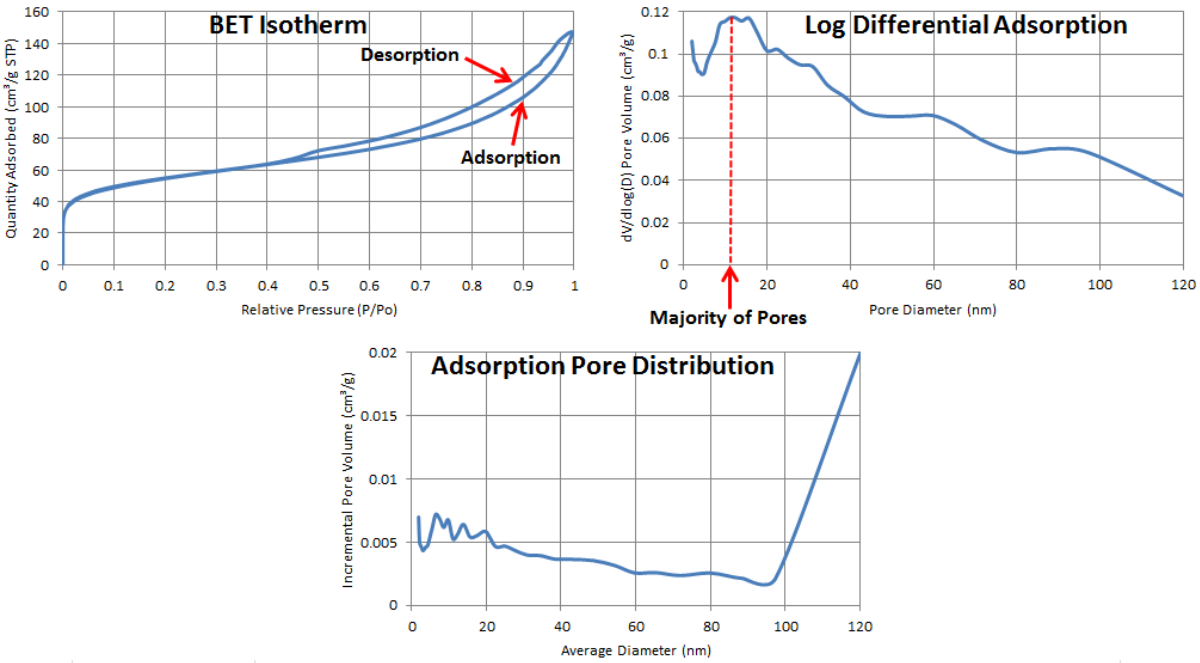

Figure 45. Nickel GDE BET Analysis Curves

9. Low Cost Uni-functional Electrodes for Flow Cells

Bi-functional Ni based GDEs are excellent durable electrodes for two electrode rechargeable zinc-air batteries. These cathodes eliminate the carbon corrosion problem, as well as greatly improving charge/discharge over-potentials, and durability. However, Ni being one of the expensive metals, make this kind of rechargeable zinc-air battery expensive compared to its generic mechanically rechargeable version. The Ni based cathode zinc-air battery has its place for vehicle application where energy density is crucial. In the case of grid energy storage, these batteries are too expensive. Therefore, a three electrode system will be developed where uni-functional OER and ORR cathodes will be utilized.

Dong Un Lee, from the lab, has experimented with different cheap OER electrodes and their galvanodynamic curves are shown in Figure 46. The full cell tests were conducted for a cathode area of 2.85cm^2. Therefore, 10mA/cm^2 would be equivalent to the values marked by the red line shown in the figure. It is clearly evident that stainless steel shows a promising OER charging voltage of 2V. This is due to the presence of electroactive oxide species in the stainless steel. Thus, one can conclude that stainless steel is a cheap and effective OER electrode that can be used for the three electrode flow cell.

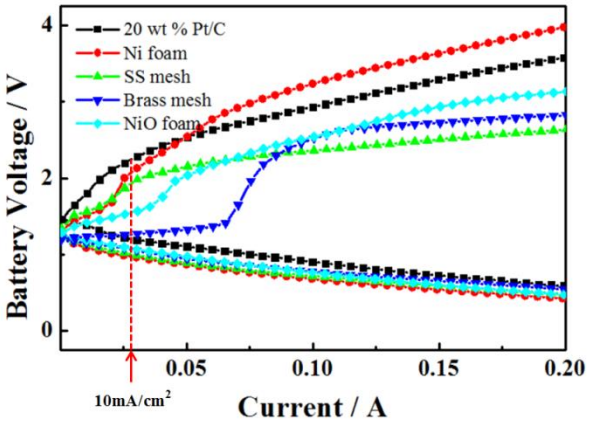

Figure 46. OER Electrodes Galvanodynamic Curves

A carbon gas diffusion electrode was fabricated using activated charcoal as the support base. Activated charcoal has a high surface area than graphite and is slightly catalytic somewhat like nickel oxide present in Ni. Not only that, it is extremely cheap making it an excellent replacement for Ni. The cathode was fabricated following the same procedures of the roll pressing technique. The galvanodynamic discharge curves were acquired and compared against that of Ni based cathodes. The performance is shown in Figure 47. There is a discrepancy between the two even though similar fabrication methods were employed.

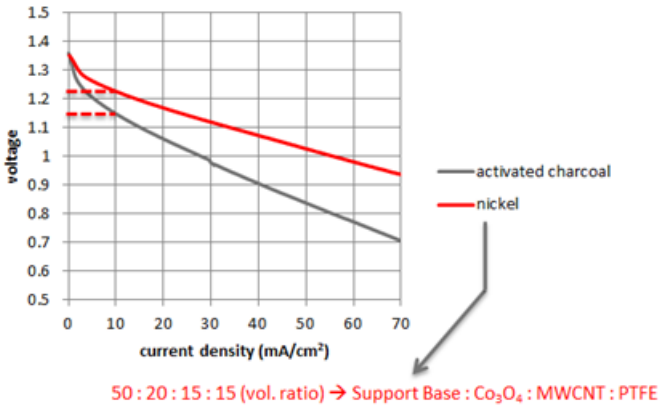

Figure 47. Comparison of Galvanodynamic Discharge Curves (Ni vs. Act. C)

To further investigate this, Ni and activated charcoal were both used as a support but with different volume ratios. The galvanodynamic curves for these different composition cathodes are shown in Figure 48. One might believe that the difference in performance between the full Ni cathode and full carbon cathode is the fact that Ni is highly conductive. This may be partially true and is evident from how the voltage slightly improves as Ni vol% is improved in the hybrid cathodes. However, this performance increase caps at 10vol% Ni as there is hardly any difference between 10vol% and 15vol% Ni hybrid cathodes. The major reason for the large difference in performance between Ni only cathode and the other carbon based cathodes is that carbon is highly hydrophobic.

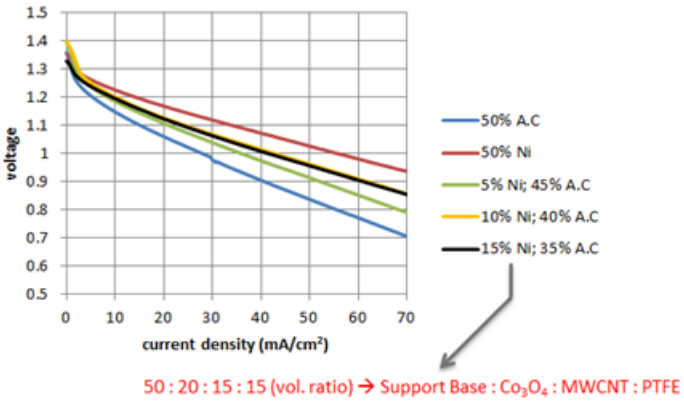

Figure 48. Comparison of Galvanodynamic Discharge Curves (Varying Ni Compositions)

The contact angle image captures for the Ni only cathode and the 15vol% Ni 35vol% C hybrid cathode is shown in Figure 49. One might believe that the PTFE in the Ni based electrodes somewhat contributes to hydrophobicity but this is true before the cathode is soaked in the KOH. As soon as it is soaked in KOH, the high voltage bias experienced at the Ni support absorbs electrolyte via electro-osmosis which is beneficial for the catalyst active hydrophilic layer. This is not possible for the carbon based electrodes due to the high hydrophobic characteristic of carbon. Therefore, the amount of electrolyte available to the catalyst active sites is limited; hence, the low voltage for the discharge curves. Even though the voltage is low, and only by 0.1V, it is overshadowed by the significant cost advantage of the carbon based electrode in grid storage applications.

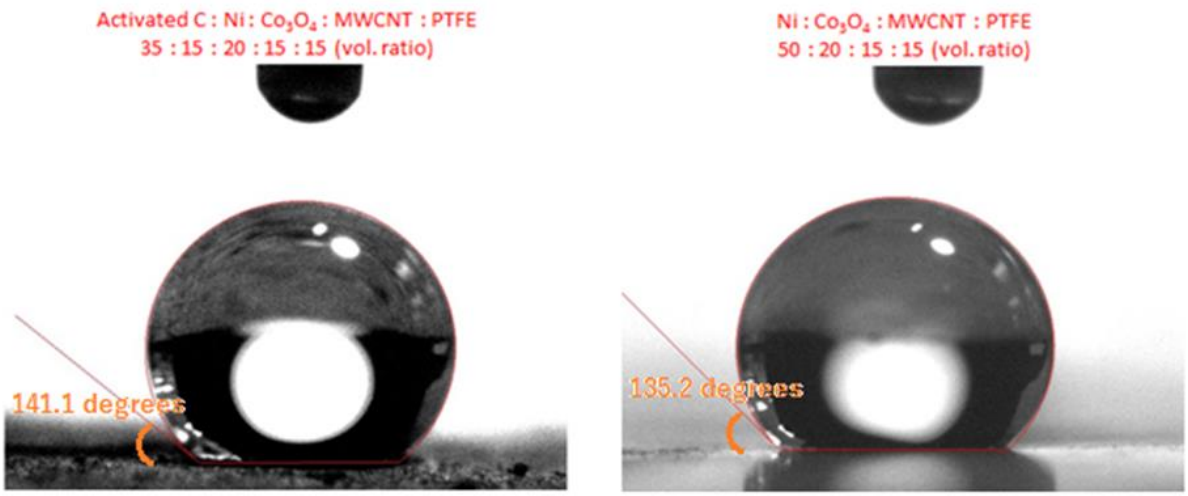

Figure 49. Contact Angle Image Captures

Now that the fabrication technique of the carbon based electrode has been finalized, one can choose a catalyst that is relatively cheap, has excellent ORR activity, and have the volume % optimized. Ali Ghorbani, from the lab, has experimented with electrolytically precipitated MnO_2 nano-powder as the catalyst for the gas diffusion electrode. MnO_2 is widely used an

ORR catalyst in basic conditions in the industry. In fact, it has better ORR activity than Co_3O_4-MWCNT. Co_3O_4-MWCNT is ideal for only bi-functional electrodes where both ORR and OER activity is required. The volume % of MnO_2 has been optimized to 3.5%. Therefore, the preferred composition of the electrode is 81.5vol% activated charcoal, 3.5vol% MnO_2, and 15vol% PTFE. The galvanodynamic discharge curve is shown in Figure 50.

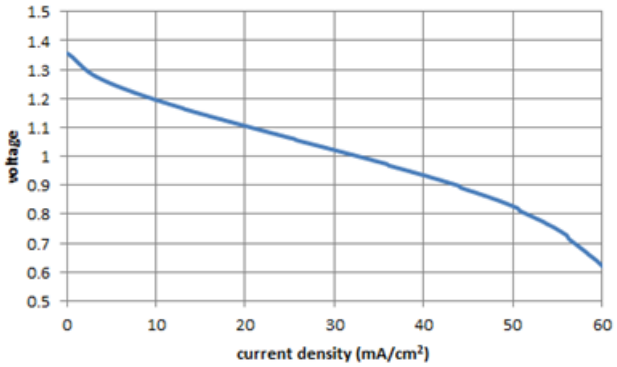

Figure 50. Galvanodynamic Discharge Curve for MnO_2 based Carbon GDE

10. Large Cell Designs: 3 Electrode Cells; Bi-functional Electrode Cells

To test the uni-functional electrodes selected in Section 9, a large cell housing that utilizes a flow system was modelled. The cell was modelled using AutoCAD by Ali Ghorbani and is shown in Figure 51. It shows a simple model with slots separating the anode and cathode. This allows for the anode and cathode to be easily mechanically replaced from the top. Electrolyte is flown from the bottom to the top so that electrodes are evenly wetted by the electrolyte. This model was transferred to ANSYS and minor changes were performed to the housing walls. A fluid domain was introduced inside the cell chamber and a mesh was created for it for CFD analysis as shown in Figure 52. The flow analysis was done using very simple assumptions. The walls were modelled as no slip smooth walls, no heat transfer was included, only k-Epsilon turbulence was included, and the liquid was treated as being continuous.

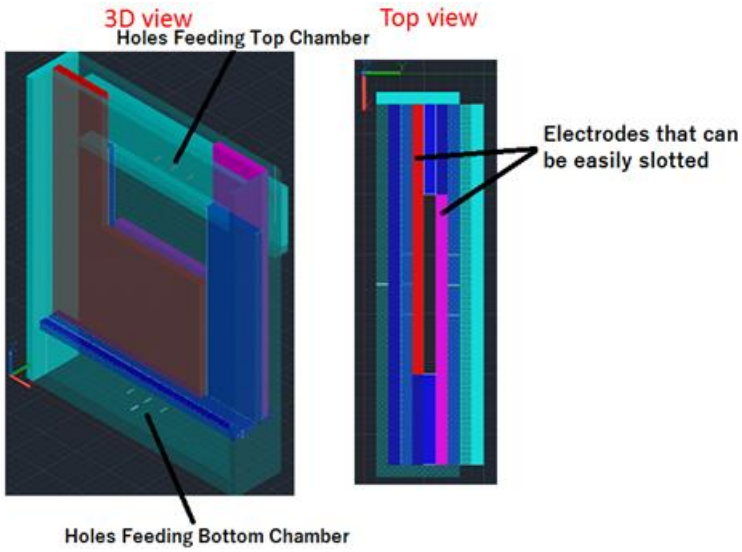

Figure 51. AutoCAD Flow Cell Models

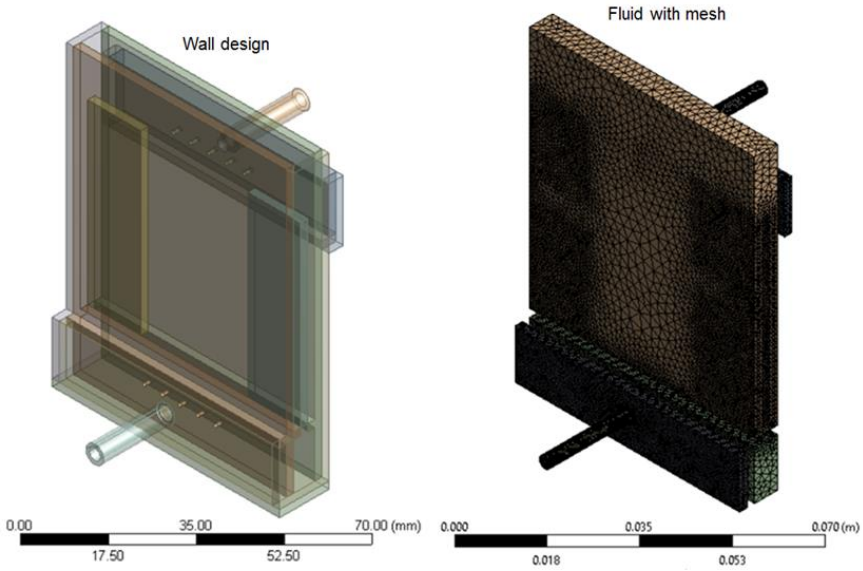

Figure 52. Flow Cell Fluid Domain Mesh

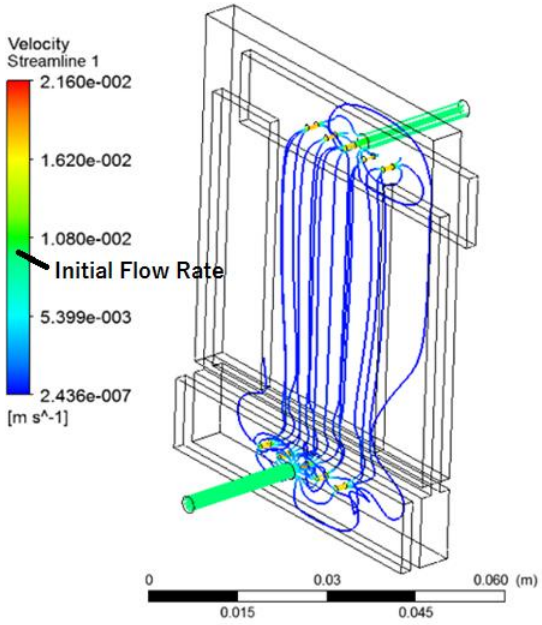

Figure 53. CFD Fluid Streams for the Flow Cell

The flow streams shown in Figure 53 look even at the center of the cell with absence of any form of turbulence. However, a 5 order of magnitude decrease in flow rate at the center of the

cell shows that further modifications need to be done to the inlet and outlet design. As the holes are too small compared to the inner chamber, there is an abrupt pressure drop; thus, the decrease in flow rate. Therefore in future models, the design will be improved to facilitate a more gradual change in the flow rate. The optimal design of the flow cell is still being engineered by Ali Ghorbani and will be completed in the near future. Figure 54 shows a schematic of the flow system, as well as one of the flow cells running. Figure 55 shows one of the newer generation of flow cells created in the lab.

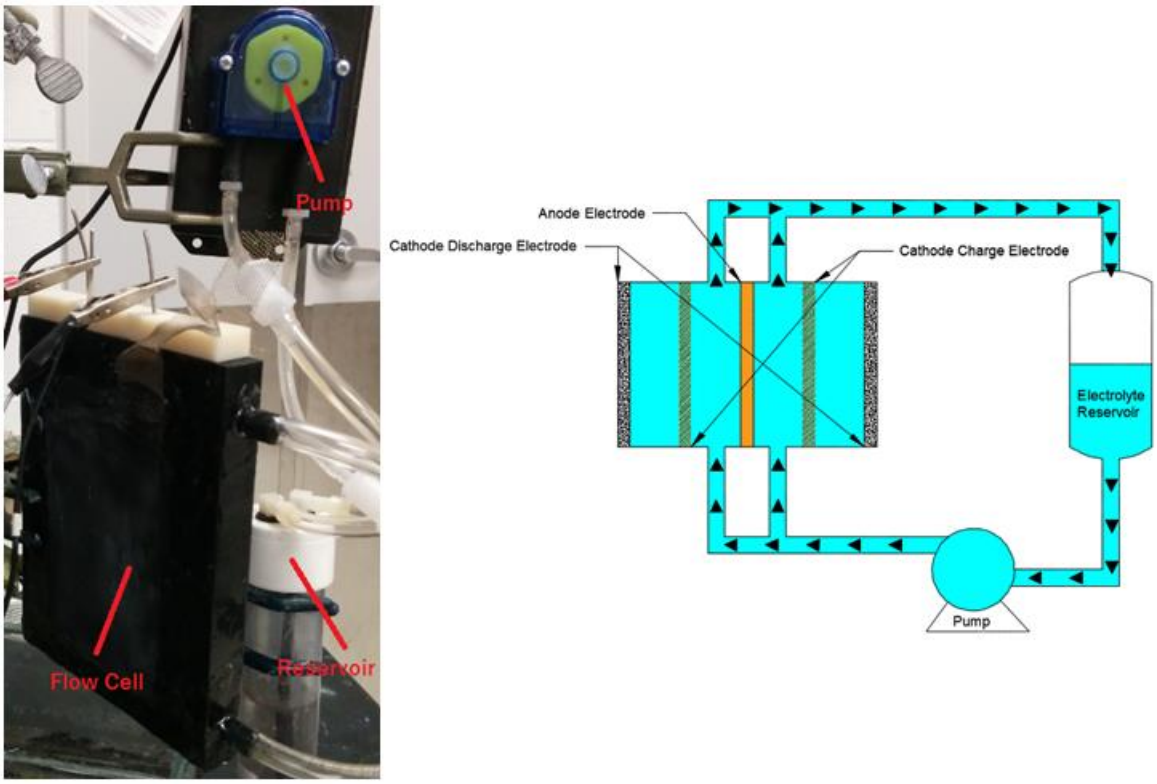

Figure 54. Flow System Schematic

Figure 55. New Flow Cells

The stainless steel OER electrode and the MnO_2 based carbon GDE were assembled into one of the flow cells. Bare copper mesh was used as the anode where zinc electrodeposition and cleaning will be conducted. This will help control the exact capacity of the anode instead of use of a bulk zinc plate which has large amount of zinc. 0.4M of $ZnCl_2$ will be dissolved in the electrolyte which will act as the zincate reserve for electroplating Zn. It should be noted that the ceramic anodes will not be utilized for this test because of the unavailability of equipment in the lab, such as big molds and furnaces, to create large area anodes. Also, the ceramic anodes have a large capacity which will take a long time to get the C/D cycles.

Hao Liu, from the lab, manually acquired 7 charge/discharge cycles using this cell setup. This is because the galvanostat/potentiostat machine has still not been setup for three electrode configuration analysis. Certain hardware changes need to be made for automatic cycling. Thus, manual cycling was done by interchanging the working lead between the OER and ORR electrode between every charge and discharge. This was done for 7 cycles. The cycling curves are shown in Figure 56. The charge and discharge voltage efficiencies are good. Zinc

was electroplated for 65mAh at 10mA/cm^2. The drop in efficiency in the capacity is due to the fact that smooth electroplated zinc is acting as the anode. This has very low porosity leading to surface dendrite formation and loss of working capacity. The drop in efficiency would be very low in the case of ceramic anodes. Further investigations will be performed in the future in the lab, utilizing both the ceramic anode and the fabricated cathodes in the flow cell. Also, greater number of cycles will be acquired once equipment is ready.

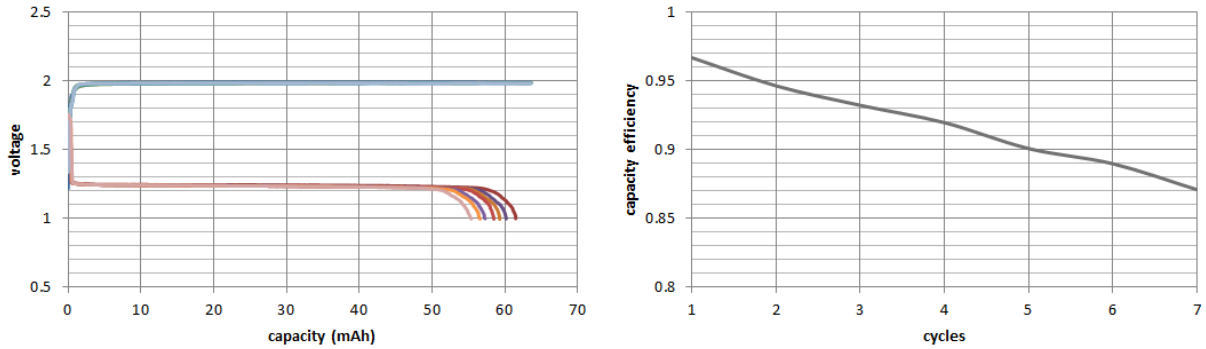

Figure 56. Zinc Cleaning Flow Cell C/D Cycles

Figure 57 shows preliminary designs for the bi-functional electrode cell housing. Five different factors were taken into account when designing this stack:

- Maximum cathode area exposed to air and thin cells to increase specific and volumetric energy density;
- Efficient cell stacking to allow for ample air flow through the cathode surfaces;
- Tight sealing to prevent electrolyte leaking;
- Gas release valves to allow for hydrogen and oxygen escaping the tightly sealed cell; and,

- Lids that can be opened to change out degraded anode and cathode and allow for easy recycling.

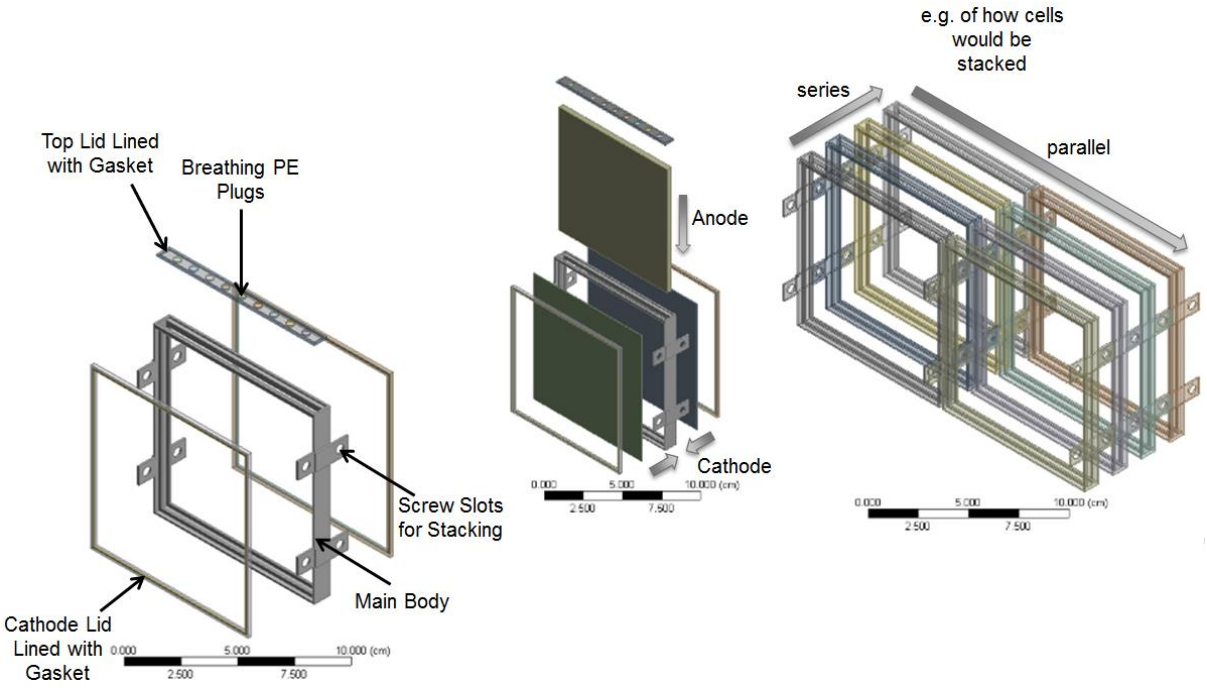

Figure 57. Bi-functional Electrode Cell Stack Preliminary Design

The cells are very thin (1cm thick) with an active cathode area of ~175cm^2/cell leading to high power and energy density. The high area is achievable due to two cathodes in one cell (back and front). The lids are lined with silicone gaskets that will ensure a tight seal when capped. The anode can be easily slotted from the top, and when needed, can also be easily replaced by opening the lids. The top lid has several holes plugged with porous polyethylene. These porous plugs can be purchased from stores such as Porex. They are hydrophobic thereby preventing electrolyte splash out, and are porous which will allow for gases such as oxygen and hydrogen to escape. The cells also feature screw slots at the edges which allow for easy stacking as shown in the figure. Air will be blown parallel to the cathode surfaces

probably with fans. Also, the air will be run through LiOH scrubbers to remove CO_2 before being circulated around the stack. Obviously, the designs have still not been finalized and further changes will need to be made before finally producing them. Once they are made, the ceramic anodes and Ni cathodes will be incorporated into them and tested individually as well as in a stack.

11. Summary

In this thesis, many of the challenges of the zinc anode, cathode, and cell packaging have been addressed. Carefully designed electrodes were developed, and their properties investigated, in order to explain any unknown phenomenon observed. The parts that were addressed in the thesis include:

- Cellulose based zinc anode;
- Ceramic anode;
- Ni cathodes made via Mechanical Press;
- Ni cathodes made via Roll Press;
- Uni-functional Cathode Electrodes;
- Three Electrode Flow Cells; and,
- Bi-functional Cathode Stack Cells.

Bismuth and indium were alloyed with all the anodes to suppress hydrogen evolution. Thick cellulose based zinc anodes were fabricated. The effect of cellulose content in these thick electrodes was investigated and the optimal quantity was concluded to be 5wt%. Performance is increased due to electrolyte absorption via the hygroscopic cellulose. However, too much cellulose can lead to anode breakage, as evident in the 10wt% cellulose anode, due to the cellulose expanding when it absorbs electrolyte. Thick ceramic anodes were prepared which have a definitive advantage of high mechanical strength over cellulose anodes. Micelles produced, by the interaction between non-polar solvent and surfactant, are the major contributors to the type of pore distribution. A complex heat treatment technique was utilized to create a continuous zinc network that is highly conductive. Ceramic anodes made from two

different non-polar solvents, decane and dodecane, were investigated via full cell testing. Both the anodes had superior voltage efficiencies compared to bulk zinc. Dendrite formation was significantly reduced and this was confirmed via SEM images. Difference between decane and dodecane is the vapor pressure; low vapor pressure of dodecane contributed to loss of micelles during the drying process leading to lower porosity. The exact over-potential of the decane based ceramic anode was recorded, which is only a fraction of that of the cathode, proving that the cathode is the major issue in performance.

Three layer Ni cathodes were prepared via mechanical press as a replacement for carbon cathodes to prevent carbon corrosion during charging. The three layers constitute: Ni screen, hydrophilic layer (50vol% Ni, 20vol% Co_3O_4, 15vol% MWCNT, 15vol% PTFE), and hydrophobic layer (80vol% Ni, 20vol% PTFE). Voltage efficiencies in the full cell were significantly improved compared to that of commercial cathodes. However, leaking occurs over-time due to the hydrophilic character of Ni coupled with electro-osmosis. A new three layer Ni cathode was fabricated to address this issue where the hydrophobic gas diffusion layer consists of a PTFE only membrane of 70% porosity. This cathode was fabricated via roll press to improve performance by increasing porosity. Three different types of the roll press fabrication were investigated. It was concluded that a cathode, where the hydrophilic layer is sandwiched between the Ni screen and PTFE film and all annealed together, gave the best result. Annealing PTFE film with the hydrophilic layer ensures full sintering and establishment of a proper three phase interface regime. Placement of Ni screen at the front of the GDE will ensure there is no water buildup at the interface between the hydrophilic layer and PTFE film. However if it is placed in between, the interface is destroyed by electro-osmosis and water and oxygen evolution during charging. 10mA/cm^2 was concluded to be a

decent current rate where minimal voltage change occurred in the lifetime of the cathode. BET analysis was conducted on the hydrophilic layer of the cathode, and a porosity of 70% by volume was calculated. The pore distribution ranged 0-120nm but most being clustered around 10nm.

Low cost uni-functional electrodes were investigated for use in a three electrode flow cell system. Stainless steel mesh has a decent charging voltage and is relatively cheap, making it ideal as an OER electrode. The carbon electrode was fabricated from activated charcoal utilizing the same roll pressing technique. Galvanodynamic performance was compared to that of the Ni based electrode, and was observed to be slightly slow. This was attributed to the hydrophobic characteristic of carbon which prevents full wetting of all the catalyst active sites. It was confirmed by contact angle images. Finally, cheap carbon electrode with electrolytically precipitated MnO_2 was fabricated with a low and effective MnO_2 volume % of 3.5%. It had greater discharge efficiency than that of Co_3O_4-MWCNT due to its greater ORR activity.

AutoCAD models were generated for the flow cell housing. This was transferred to ANSYS for CFD analysis. Stream flows were even but there was a significant drop in pressure at the center of the chamber. Design implementations to address this problem will be conducted in the future. The SS mesh OER electrode and MnO_2 based ORR cathode were tested in the flow cell. The cell was manually cycled by interchanging potentiostat working leads between the OER and ORR electrode in between C/D cycles. Decent voltage efficiencies are observed; however, drop in capacity efficiency over-time is noticed due to dendritic shape change in the electroplated zinc. Future tests will involve ceramic anode utilization and

longer cycles will be acquired. Large bi-functional electrode cell housing was modelled. The design includes 1cm thin cells with double sided cathode of total area ~175cm^2, maximizing oxygen input and energy density. Lids lined with gaskets ensure tight sealing and leave the possibility for electrode recycling. PE plugs prevent pressure build up due to gas evolution. Also, screw slots allow for efficient cell stacking allowing for ample air to flow parallel to cathode surfaces. These stack designs need to be further improved before finalizing production, after which the anodes and cathodes will be tested in them.

References

[1] "Worldometers," [Online], Available: http://www.worldometers.info/world-population/#growthrate, [Accessed April 2014].

[2] "Why did fossil fuels become so popular?," Mitsubishi Heavy Industries Ltd. Global, [Online], Available: https://www.mhi-global.com/discover/earth/issue/history/history.html, [Accessed April 2014].

[3] B. Scrosati, J. Garche, "Synthesis and Characterization of Silicon Nanoparticles Inserted into Graphene Sheets as High Performance Anode Material for Lithium Ion Batteries," Journal of Power Sources, vol. 195, no. 9, pp. 2419-2430, 2010.

[4] F. T. Wagner, B. Lakshmanan, M. F. Mathias, "Electrochemistry and the Future of the Automobile," Journal of Physical Chemistry Letters, vol. 1, no. 14, pp. 2204-2219, 2010.

[5] B. Dunn, H. Kamath, J. M. Tarascon, "Electrical energy storage for the grid: a battery of choices," Science, vol. 334, no. 6058, pp. 928-935, 2011.

[6] M. Skyllas-Kazacos, M. H. Chakrabarti, S. A. Hajimolana, F. S. Mjalli, M. Saleem, "Progress in Flow Battery Research and Development," Journal of the Electrochemical Society, vol. 158, no. 8, R55-R79, 2011.

[7] G. L. Soloveichik, "Battery Technologies for Large-Scale Stationary Energy Storage," Annual Review of Chemical and Biomolecular Engineering, vol 2, pp. 503-527, 2011.

[8] M. Armand, J. M. Tarascon, "Building better batteries," Nature, vol. 451, no. 7179, pp. 652-657, 2008.

[9] M. Broussely, J. P. Planchat, G. Rigobert, D. Virey, G. Sarre, "Lithium-ion batteries for electric vehicles: performances of 100 Ah cells," Journal of Power Sources, vol. 68, no. 1, pp. 8-12, 1997.

[10] B. Kennedy, D. Patterson, S. Camilleri, "Use of lithium-ion batteries in electric vehicles," Journal of Power Sources, vol. 90, no. 2, pp. 156-162, 2000.

[11] G. Girishkumar, B. McCloskey, A. C. Luntz, S. Swanson, W. Wilcke, "Lithium−Air Battery: Promise and Challenges," Journal of Physical Chemistry Letters, vol. 1, no. 14, pp. 2193-2203, 2010.

[12] K. Kinoshita, E. Society, "Electrochemical Oxygen Technology," Wiley, 1992.

[13] J. F. Parker, C. N. Chervin, E. S. Nelson, D. R. Rolison, J. W. Long, "Wiring zinc in three dimensions re-writes battery performance—dendrite-free cycling," Energy & Environmental Science, vol. 7, no. 3, pp. 1117-1124, 2014.

[14] L. Jörissen, “Bifunctional oxygen/air electrodes,” Journal of Power Sources, vol. 155, no. 1, pp. 23-32, 2006.

[15] R. Ahmed, K. Shah, A. Ameen, B. Shokouhi, M. Liem, “Prototype Construction,” Nanotechnology Engineering Fourth Year Design Project Final Report, University of Waterloo, pp. 18-20, 2013.

[16] J. S. Lee, S. T. Kim, R. Cao, N. S. Choi, M. Liu, K. T. Lee, J. Cho, “Metal–Air Batteries with High Energy Density: Li–Air versus Zn–Air,” Advanced Energy Materials, vol. 1, pp. 34-50, 2011.

[17] K. Fehrenbacher, "Fluidic shows a peek of its metal air batteries for off and on the grid," Gigaom, [Online], Available: https://gigaom.com/2013/03/01/fluidic-shows-a-peek-of-its-metal-air-batteries-for-off-and-on-the-grid/, [Accessed April 2014].

[18] J. Lenos, Photography Collection, 2014.

[19] S. Müller, F. Holzer, O. Haas, “Optimized zinc electrode for the rechargeable zinc–air battery,” Journal of Applied Electrochemistry, vol. 28, no. 9, pp. 895-898, 1998.

[20] D. R. Rolison, J. F. Parker, J. W. Long, “Zinc electrodes for batteries,” Patent US 13/832,576, May 29, 2014.

[21] “Standard Reduction Potentials in Aqueous Solution at 25°C,” [Online], Available: http://www.chemeddl.org/services/moodle/media/QBank/GenChem/Tables/EStandardTable.htm, [Accessed March 2015].

[22] T. I. Devyatkina, Y. L. Gun'ko, M. G. Mikhalenko, “Development of Ways To Diminish Corrosion of Zinc Electrode,” Russian Journal of Applied Chemistry, vol. 74, no. 7, pp. 1122-1125, 2001.

[23] C. W. Lee, K. Sathiyanarayanan, S. W. Eom, M. S. Yun, “Novel alloys to improve the electrochemical behavior of zinc anodes for zinc/air battery,” Journal of Power Sources, vol. 160, no. 2, pp. 1436-1441, 2006.

[24] C. Zhang, J. M. Wang, L. Zhang, J. Q. Zhang, C. N. Cao, “Study of the performance of secondary alkaline pasted zinc electrodes,” Journal of Applied Electrochemistry, vol. 31, no. 9, pp. 1049-1054, 2001.

[25] C. W. Lee, K. I. Sathiyanarayanan, S. W. Eom, H. S. Kim, M. S. Yun, “Novel electrochemical behavior of zinc anodes in zinc/air batteries in the presence of additives,” Journal of Power Sources, vol. 159, no. 2, pp. 1474-1477, 2006.

[26] P. Sapkota, H. Kim, “Zinc-air fuel cell, a potential candidate for alternative energy,” Journal of Industrial and Engineering Chemistry, vol. 15, no. 4, pp. 445-450, 2009.

[27] P. Sapkota, H. Kim, "An experimental study on the performance of a zinc air fuel cell with inexpensive metal oxide catalysts and porous organic polymer separators," Journal of Industrial and Engineering Chemistry, vol. 16, no. 1, pp. 39-44, 2010.

[28] F. R. Mclarnon, E. J. Cairns, "The Secondary Alkaline Zinc Electrode," Journal of the Electrochemical Society, vol. 138, no. 2, pp. 645-656, 1991.

[29] T. Hibino, K. Kobayashi, "Electronic Supplementary Information for Intermediate-temperature alkaline fuel cells with non-platinum electrodes," Journal of Materials Chemistry A, vol. 1, pp. 7019-7022, 2013.

[30] H. H. Simmons, R. D. Smith, "A New Synthesis of Cyclopropanes," J. Am. Chem. Soc., vol. 81, no. 16, pp. 4256-4264, 1959.

[31] "What is the Difference Between Carbon Paper and Carbon Cloth Based Gas Diffusion Layers (GDL)?," Fuel Cells Etc, 8 March 2013. [Online], Available: http://fuelcellsetc.com/2013/03/comparing-gas-diffusion-layers-gdl/, [Accessed April 2014].

[32] "Multiphase flow in porous gas diffusion layer (GDL)," UCDAVIS College of Engineering, [Online], Available: http://mae.engr.ucdavis.edu/jwpark/DavisSite/pages/research.html, [Accessed March 2015].

[33] "Determination of the surface area by the BET method," Quantum Coherence Lab University of Basel, [Online], Available: http://zumbuhllab.unibas.ch/pdf/talks/080425_Tobias_BET.pdf, [Accessed April 2014].

[34] G. Lin, T. V. Nguyen, "Effect of Thickness and Hydrophobic Polymer Content of the Gas Diffusion Layer on Electrode Flooding Level in a PEMFC," Journal of The Electrochemical Society, vol. 10, no. 152, pp. A1942-A1948, 2005.

[35] Z. L. Wang, et al., "Oxygen electrocatalysts in metal-air batteries: from aqueous to nonaqueous electrolytes," Chemical Society Reviews, vol. 43, no. 22, pp. 7746-86, 2014.

[36] M. R. Miah and T. Ohsaka, "Two-Step Four-Electron Reduction of Molecular Oxygen at Iodine-Adatoms-Modified Gold Electrode in Alkaline Media," International Journal of Electrochemical Science, vol. 7, pp. 697-710, 2012.

[37] R. Donkers, L. Liao, L. Deakin, C. Backhouse, "Electrochemical Characterization of Platinum Nanoelectrocatalysts Supported on Carbon Nanotubes," Nanotechnology Engineering Program, University of Waterloo, 2013.

[38] Y. Xu, X. Xu, G. Li, Z. Zhang, G. Hu, Y. Zheng, "Experimental Research of Liquid Infiltration and Leakage in Zinc Air Battery," International Journal of Electrochemical Science, vol. 8, pp. 11805-11813, 2013.

[39] C. D. Tran, "Investigation of Oxygen Reduction on the Carbon Gas-Diffusion Electrode in Non-Aqueous Electrolyte," University of Massachusetts Boston ScholarWorks at UMass Boston, Boston, 2011.

[40] J. F. Drillet, M. Adam, S. Barg, A. Herter, D. Koch, V. Schmidt, M. Wilhelm, "Development of a Novel Zinc/Air Fuel Cell with a Zn Foam Anode, a PVA/KOH Membrane and a MnO_2/SiOC-Based Air Cathode," ECS Trans., vol. 28, no. 32, pp. 13-24, 2010.

[41] R. Ahmed, "Environmental Scanning Electron Microscopy," Chemical Engineering Program, University of Waterloo, 2014.

[42] L. Reimer, "Introduction," Scanning Electron Microscopy: Physics of Image Formation and Microanalysis, Springer Series in Optical Sciences, vol. 45, pp. 2, 1998.

[43] "Static volumetric gas adsorption," University of Oxford, [Online], http://saf.chem.ox.ac.uk/operating-principles-3.aspx, [Accessed March 2015].

[44] "Drop Shape Analyzer – DSA100," KRUSS Advancing Your Surface Science, [Online], Available: http://www.kruss.de/products/contact-angle/dsa100/drop-shape-analyzer-dsa100/, [Accessed March 2015].

[45] R. Ahmed, K. Shah, A. Ameen, B. Shokouhi, M. Liem, "Design Specifications," Nanotechnology Engineering Fourth Year Design Project Final Report, University of Waterloo, G-6, 2013.

[46] R. Ahmed, K. Shah, A. Ameen, B. Shokouhi, M. Liem, "Design Specifications," Nanotechnology Engineering Fourth Year Design Project Final Report, University of Waterloo, G-7, 2013.

[47] Limited-Vision-Stock, "Cracks 01," DeviantArt, [Online], Available: http://limited-vision-stock.deviantart.com/art/Cracks-01-196969796, [Accessed March 2015].

[48] D. U. Lee, "Advanced Nanostructured Bi-functional Air Electrode for Rechargeable Zinc-Air Batteries," Chemical Engineering Program, University of Waterloo, 2014.